Quaternary Science Reviews 222 (2019) 105899

Contents lists available at ScienceDirect

Quaternary Science Reviews

journal homepage: www.elsevier.com/locate/quascirev

n-Alkyl nitriles and compound-specific carbon isotope analysis of lipid combustion residues from Neanderthal and experimental hearths: Identifying sources of organic compounds and combustion temperatures

Margarita Jambrina-Enríquez*, Antonio V. Herrera-Herrera, Caterina Rodríguez de Vera, Lucia Leierer, Rory Connolly, Carolina Mallol

Archaeological Micromorphology and Biomarker Research Lab, Instituto Universitario de Bio-Orgánica "Antonio González" (IUBO), Universidad de La Laguna (ULL), Avda. Astrofísico Fco. Sánchez, 2, 38200 La Laguna, Tenerife, Spain

ARTICLE INFO

Article history:
Received 28 February 2019
Received in revised form
11 August 2019
Accepted 21 August 2019
Available online 6 September 2019

Keywords:
Plant lipids
Combustion structures
Biomarkers
Fatty acids
Archaeology
Pleistocene
Europe
Stable isotopes
Organic geochemistry

ABSTRACT

Molecular and isotopic approaches offer the chance to identify combustion residues and substrate components of archaeological combustion features to infer past fire-related activities. Analysis of fatty acid methyl esters by gas chromatography-combustion-isotope ratio mass spectrometry have been successfully used to distinguish among different animal fat groups. However, plant oils from different tissues have not been widely investigated even though organic residues from leaf, root, and wood tissues are preserved in sediments from archaeological combustion structures. Our analyses of plant residues from controlled laboratory heating sequences and experimental hearths involving wood and animal residues, provide references to discern anatomical parts of fresh and charred plants and to differentiate contributions of terrestrial plants and animal sources in open air hearths. This information is compared with charred organic residues from combustion structures from three Middle Palaeolithic sites: El Salt (Spain), Abric del Pastor (Spain) and Crvena Stijena (Montenegro). The occurrence of *n*-alkyl nitriles in our samples corroborates their potential as combustion temperature biomarkers and the $\delta^{13}C_{16:0}$ and $\delta^{13}C_{18:0}$ values allow us differentiate between charred and fresh plant anatomical parts and between fresh plant oils and animal fats.

© 2019 The Authors. Published by Elsevier Ltd. This is an open access article under the CC BY-NC-ND license (http://creativecommons.org/licenses/by-nc-nd/4.0/).

1. Introduction

Combustion features are among the most commonly occurring anthropogenic features in archaeological sites from all regions and time periods and are particularly relevant to Middle Palaeolithic research given their prominence in the archaeological record (Roebroeks and Villa, 2011). Stratigraphically, they are composed of a combustion substrate (commonly black layers which represent charred soil matter beneath the fire e.g., leaves, seeds, roots) overlain by one or more layers of burnt residues (often white or grey ashy layers) (Mallol et al., 2017). Common organic burnt constituents of archaeological combustion features include animal (animal fat-derived char, burnt bone) and plant components (charcoal, char, charred plant tissues) (Mallol et al., 2017).

The application of isotopic organic chemistry towards identification of combustion residues and substrate components can provide a robust dataset to infer past fire-related activities such as cooking or biomass burning. Cooking is a common use of fire, hypothetically since the Palaeolithic (Clark and Harris, 1985; Karkanas et al., 2007; Henry, 2017; Wrangham, 2017) and anthropogenic biomass burning has been recognised in South African Middle Stone Age sites (i.e. maintenance fires involving burning of plant bedding for hygiene) (Goldberg et al., 2009; Wadley et al., 2011; Miller et al., 2013). Other studies have proposed the use of fire for ecosystem management in East Asia since the earliest human colonization of the region (Beaufort et al., 2003; Thevenon et al., 2004) and suggested the lack of this behaviour in Middle and Upper Palaeolithic Europe (Daniau et al., 2010).

* Corresponding author.
E-mail addresses: mjambrin@ull.edu.es (M. Jambrina-Enríquez), avherrer@ull.edu.es (A.V. Herrera-Herrera), crodrive@ull.edu.es (C. Rodríguez de Vera), lleierer@ull.es (L. Leierer), rconnoll@ull.es (R. Connolly), cmallol@ull.edu.es (C. Mallol).

https://doi.org/10.1016/j.quascirev.2019.105899
0277-3791/© 2019 The Authors. Published by Elsevier Ltd. This is an open access article under the CC BY-NC-ND license (http://creativecommons.org/licenses/by-nc-nd/4.0/).

The potential of compound-specific $\delta^{13}C_{16:0}$ and $\delta^{13}C_{18:0}$ stable isotope analysis to distinguish between different types of animal fat has been demonstrated in a number of publications targeting organic residues encrusted on archaeological pottery (Dudd et al., 1999; Craig et al., 2007, 2011; Lucquin et al., 2016), or present in burned and cemented sand (Buonasera et al., 2015) or combustion structures (March, 2013; Choy et al., 2016) by comparing with the equivalent isotopic ratios in fresh animal-derived fat. However, the identification of plant oils in archaeological residues is scarce and mainly focused on pottery (Spangenberg et al., 2006; Steele et al., 2010). As a result, the reference plant oil database of $\delta^{13}C_{16:0}$ and $\delta^{13}C_{18:0}$ values is largely limited to fresh seed oils (Woodbury et al., 1998; Spangenberg and Ogrinc, 2001; Steele et al., 2010), while only a few studies incorporate fresh C_3-leaf oils (Chikaraishi et al., 2004a,b).

Steele et al. (2010) reported $\delta^{13}C_{16:0}$ and $\delta^{13}C_{18:0}$ values of fresh almond, argan, olive, sesame, walnut and moringa oils lying within the range of values generally accepted for ruminant and porcine adipose (Craig et al., 2011). However, not all the $\delta^{13}C_{16:0}$ and $\delta^{13}C_{18:0}$ values of seed oils lie in the range of animal fats. For example, depleted carbon isotopes are reported for cork-oak acorn oils from Spain (Recio et al., 2013) and for acorn and chestnut oils from Japan (Lucquin et al., 2018). The data gathered by Recio et al. (2013) also showed that cork-oak acorn oils are isotopically depleted in ^{13}C (~5‰) compared to fat from pigs feeding naturally on winter acorns and grass. While isotopic ratios in fresh seed oils are used to discern between plant or animal fat in archaeological organic residues on pottery (Steele et al., 2010), fresh and charred plant components of archaeological combustion structures, including leaf, wood and root residues are rarely considered despite being common organic components of combustion substrates and residues. To discern between biomass burning and cooking practices involving animal-derived elements, more compound-specific stable isotope analysis of $\delta^{13}C_{16:0}$ and $\delta^{13}C_{18:0}$ on plant oils (including fresh and charred plant tissues) are necessary.

Interestingly, emissions from meat cooking experiments (Rogge et al., 1991) and biomass burning (especially from smouldering, Oros and Simoneit, 2001a; Simoneit et al., 2003) are an important source for nitrogen-containing organic compounds as *n*-alkyl nitriles which can be applied as useful biomarkers (Simoneit et al., 2003). Simoneit et al. (2003) proposed that fatty acids react with ammonia to produce nitriles and amides during combustion. Despite their potential as biomarkers, they have not been widely considered in the sedimentary record from archaeological sites. Recent studies have detected and identified *n*-alkyl nitriles on archaeological sediments dating to 5 ka BP (Wang et al., 2017) and ranging from ≈52 to 109 ka BP (Collins et al., 2017) demonstrating their resistance to degradation.

To investigate further, we conducted laboratory and field experiments with different anatomical parts of *Celtis australis* L. *C. australis* (European nettle tree or Mediterranean hackberry) is a deciduous tree (Cannabaceae family, Sytsma et al., 2002) native of the Mediterranean region and found in dry rocky settings (Costa et al., 1998). In the Mediterranean region, phytoliths (Mallol et al., 2013; Rodríguez-Cintas and Cabanes, 2015) and seeds (Akazawa, 1987; Messager et al., 2010; Mallol et al., 2013; García Moreno et al., 2014; Allué et al., 2015) of *C. australis* have been widely recorded in sediments from Neanderthal sites. Moreover, given the broad geographic distribution and adaptability to dry conditions of *Celtis* sp., charcoal fragments have been identified in South African Middle Stone Age sites (e.g. Sibudu Cave, Hall et al., 2014). We also included additional plant parts (needles and branches) from the Pinaceae family-conifers (*Pinus canariensis)* to examine plant species effects on the isotopic composition (Pedentchouk et al., 2008).

We performed controlled laboratory heating sequences at 60, 150, 250 and 350 °C using leaves, wood (bark and xylem), roots and seeds and analysed compound-specific stable isotopes of fatty acids to determine if $\delta^{13}C_{16:0}$ and $\delta^{13}C_{18:0}$ could be used to discern anatomical parts of fresh and charred plants and to construct a small database of present-day standards. We also performed experimental open fires (experimental hearths) using *Celtis* wood as fuel on a substrate of *Celtis* leaves and on unvegetated sediment and a combination of *Celtis* wood with animal parts (rabbit). We analysed sedimentary $\delta^{13}C_{16:0}$ and $\delta^{13}C_{18:0}$ from these contexts to differentiate contributions of terrestrial and animal sources in open air hearths. Moreover, we selected combustion features from three Neanderthal sites to evaluate preservation and contribution of animal fat and plant oils using compound-specific stable isotopes of *n*-$C_{16:0}$ and *n*-$C_{18:0}$ fatty acids. The sites are chronologically framed within Marine Isotope Stages MIS 5, MIS 4 and MIS 3, and located in the western (El Salt and Abric del Pastor, Spain) and eastern (Crvena Stijena, Montenegro) Mediterranean region.

Additionally, since average temperatures associated with black layers of experimental combustion features have been reported to fall below 400 °C (Mallol et al., 2013) and *n*-alkyl nitriles have been found after laboratory thermal treatment at 300–350 °C (Ishiwatarii et al., 1992; Simoneit et al., 2003), *n*-alkyl nitriles were examined to evaluate their preservation potential in experimental and archaeological hearths to be used as a proxy for combustion temperature.

The objectives of this study were (a) to discern anatomical parts of fresh and charred plants using $\delta^{13}C_{16:0}$ and $\delta^{13}C_{18:0}$ values, (b) to test whether coupling modern $\delta^{13}C_{16:0}$ and $\delta^{13}C_{18:0}$ values of plant oils and animal fats with organic residues from Neanderthal hearths could help differentiate between animal and plant contributions (c) to evaluate the source and preservation of *n*-alkyl nitriles in modern plant references and in hearths from Neanderthal sites.

2. Materials and methods

2.1. Modern plant samples

Different anatomical parts of *Celtis australis* L. tree (leaves, lateral roots -1cm, branches of 3 cm diameter - xylem and bark and dried seeds) were collected near the archaeological site of El Salt (Alcoy, Spain) (38°41′14″N, 0°30′32″W, 726 m above sea level). Samples were rinsed with distilled water and then oven-dried at 60 °C for 24 h. Further experimental combustion under laboratory controlled conditions (ramp rate of 26 °C/min, oxygen-limited supply, 1 h of combustion at 150 °C, 250 °C, 350 °C and 450 °C) were performed in a muffle furnace using 0.5–1 g (seeds), 4 g (leaves and roots) and 20 g (bark and xylem) of fresh material. Leaves were also charred at 250 °C during 3 and 5 h (see Jambrina-Enríquez et al., 2018 for more details). These samples were taken as reference for charred ground (leaves, roots, seeds and branches −bark and xylem) beneath the fire (sedimentary black layers in combustion structures).

Additional plant tissues (needles and branches of 3 cm diameter) from the Pinaceae family - conifers (*Pinus canariensis*) were collected in Cruz de Tea (Tenerife) in an area away from sources of pollution (28°8′26.2″N, 16°36′2.4″W, 980 m a.s.l.) with permission of the Consejería de Medio Ambiente del Cabildo de Tenerife. The fresh wood and needles were also charred at 350 °C (1 h).

2.2. Experimental hearths

We performed three experimental open hearths using *Celtis* wood as fuel in the immediate surroundings of El Salt. The first experimental hearth was made in 2010 and samples were collected three years later (NFT10-1-T3). This hearth was made on a dry, unvegetated, loose calcareous sediment with 12.5 kg of *Celtis* wood and rabbit meat, inners and skin were tossed in the flames. Rabbit meat was used in this experiment because rabbit bone is prominent in faunal assemblages from western and eastern Mediterranean Palaeolithic sites (Hockett and Haws, 2002) and abundant burnt rabbit bone specimens have been recovered from El Salt (Pérez, 2014, 2015). Pine needles were used as tinder. Thermocouples were placed at the surface and 2 cm below the surface to monitor the influence of temperature on the sedimentary substrate. The hearth was burning for approximately 2 h. Peak surface temperature reached 740 °C, and 418 °C at 2 cm below the surface. From the remains of this hearth, we collected a fragment of *Celtis* charcoal and four sediment samples from top to base of a 7 cm profile: 1) white layer - WL (combustion residues: wood ash, 4 cm of thickness), 2) black layer - BL (charred ground beneath the hearth, 1 cm of thickness), 3) brown layer – CM (combustion substrate, 1 cm of thickness), 4) natural substrate (sediment without apparent thermal alteration).

Two additional experimental hearths were made in 2017 (NFT17) using *Celtis* wood as fuel and without any animal input. The first hearth (NFT17-H1) consisted in *Celtis* wood fuel over a bed of *Celtis* leaves and the black (charred leaf samples) and white (a mixture of leaf and wood ashes) layers were sampled. The second hearth (NFT17-H2) was made on a dry, unvegetated, and partially consolidated calcareous sediment. Since we were only interested in collecting ash samples, thermocouples were not used on these two hearths.

All the samples were collected with sterilised metal tools, wrapped in aluminium foil, and stored in plastic bags in a freezer (−20 °C) until further treatment. After freeze-drying, the samples were crushed and homogenised with an agate mortar.

2.3. Archaeological samples

Samples from archaeological combustion structures were collected using sterilised metal tools, wrapped in aluminium foil, and stored in plastic bags in a freezer (−20 °C) until further treatment and analysis.

The sites studied are El Salt – Spain (38°41′14″N, 0°30′32″W, 726 m a.s.l.), Abric del Pastor – Spain (38°42′47.7″N, 0°29′40.8″W, 820 m a.s.l.) and Crvena Stijena – Montenegro (42°46′40.4″N, 18°28′53.9″E, 800 m a.s.l.). In El Salt we selected four black layers (BL1, BL2, BL3, and BL4) and one white layer (WL) from combustion structure H50, located in the stratigraphic unit (S.U.) Xb. Unit X, which is divided into units Xa and Xb, has been dated to around 50 ka BP (Galván et al., 2014). In unit Xb, close to the Paleocene limestone wall, two clusters of combustion structures can be found, the inner and the outer cluster (Leierer et al., 2019). H50 belongs to the outer cluster. It rests on and is surrounded by brown clayey-silty sediment and is partially overlain by two combustion structures: H53 and H52 (Leierer et al., 2019). The H50 black layer (BL) is approximately 90 cm in diameter, bowl-shaped and contains dark and greasy sediment (Leierer et al., 2019). Biomarker samples H50–BL1, H50–BL2, and H50–BL3 were taken towards the base of the BL, while H50–BL4 was taken from the surface of the BL. The white layer (H50–WL) is represented by cobble-shaped imprints on the surface of the BL, filled with ashy sediment (Leierer et al., 2019).

All of the combustion features from Abric del Pastor included in this study (H9, H13, H15, H16, and H17) were excavated in S.U. IV. This stratum is composed of clast-supported, limestone cobble beds (IVa, IVe and IVg) which alternate with laterally discontinuous matrix-supported, fine-grained, calcareous sandy-gravelly deposits (IVb, IVd, and IVf) (Machado et al., 2013). Subunit IVc is composed of large boulders and angular cobbles with very little fine material, resulting from one or more significant roof collapse events. Current anthracological and faunal evidence tentatively frame the sequence between MIS 5 and 4 (Machado et al., 2013). Combustion feature H15 comes from the surface of subunit IVc, the roof collapse deposit, and is characterised by a small concentration of thermally altered limestone in association with fragments of charcoal and burnt bone. Combustion features H9, H13, H14, and H16 were recorded during the excavation of subunit IVd, a poorly sorted sandy gravelly deposit. H17 comes from subunit IVf which is a sandy gravelly deposit similar in composition to IVd, but with a slightly higher proportion of medium and coarse gravel. H17 was recorded in the field as a thin concentration of ashy sediment overlying a massive black layer.

In Crvena Stijena we collected four samples: two black layer samples (CS-BL10 and CS-BL11) from a dense black lens with a greasy texture and one ash layer sample (CS-WL6) overlying a black layer (CS-BL8). All of the combustion features belong to S.U. XXIV (MIS 5e, 90–70 ka BP), a 2.3 m-thick layer of fine sandy gravel and coarse sand with charcoal, ash, burnt and unburnt bone fragments and stratified combustion features (Morley, 2007).

2.4. Lipid extraction, separation, and analysis

Lipids from 0.3 to 2 g of plant tissues and 2–5 g of sediment were extracted by three 30 min ultrasonications rounds in 10–50 mL of dichloromethane/methanol (DCM:MeOH, 9:1 v/v). The extracts were centrifuged (10 min at 4700 rpm), filtered through a glass wool filter and fractionated on a silica gel column (1 g silica and 0.1 g sand, previously calcined at 450 °C during 10 h) into different polarity fractions (Jambrina-Enríquez et al., 2018). A low/medium polarity fraction (LPF) containing ketones, *n*-alkyl nitriles, *n*-alkyl aldehydes and fatty acid methyl esters (FAMEs) which eluted with DCM (2 column's dead volume, 3.5 mL) and a high polarity fraction (HPF) containing fatty acids (FAs) which eluted with ethyl acetate (EtOAc) (2 column's dead volume, 3.5 mL).

After evaporation under a N_2 flow, the residue of the LPF fraction was reconstituted in 50 μL of DCM with a final concentration of 8 mg/L of 5α-androstane (purity ≥ 99.9%) as internal standard (IS) for injection in the GC-MS system. The free fatty acids (HPF) were derivatised to their respective FAMEs to determine their carbon isotope ratios. In summary, 1/3 of HPF was dissolved in sulfuric methanol solution (5 mL methanol and 400 μL sulfuric acid) and heated at 70 °C for 240 min. After that, the solution was neutralised with 10 mL of saturated bicarbonate solution. To extract the FAMEs, 3 mL of hexane were added to the methanol solution and following vigorous shaking (the FAME extraction was repeated three times). Methyl nonadecanoate ($C_{19:0}$, purity ≥ 98%) was used as IS (8 mg/L) and the residue obtained after evaporation under a N_2 flow was reconstituted in 10 μL of EtOAc and 40 μL of hexane (see Jambrina-Enríquez et al., 2018 for more details).

Samples were analysed and quantified by gas chromatography with a coupled mass-selective detector (GC-Agilent 7890B, MSD Agilent 5977A) equipped with an HP-5MS capillary column (30 m length x 0.25 mm i.d., 0.25 μm film thickness), at the Archaeological Micromorphology and Biomarker Research Laboratory (University of La Laguna, Spain). The GC was programmed to an initial temperature of 70 °C for 2 min heated with a heating rate of 12 °C/min to 140 °C and a to final temperature of 320 °C with a heating rate of 3 °C/min and held for 15 min, with Helium as the carrier gas (with a

flow of 2 mL/min). The multimode injector was held at a split ratio of 5:1 at an initial temperature of 70 °C during 0.85 min and heated to 300 °C at a programmed rate of 720 °C/min. All measurements were done in duplicate.

LPF compounds were identified based on characteristic ions and by comparison of their mass spectra with those of reference to the NIST Mass Spectra Database v.14. For fatty acids, a 37 component FAME mix C_4-C_{24} standard (concentration in DCM varied from 200 to 600 mg/L) and fatty acids $C_{26:0}$, $C_{28:0}$ and $C_{30:0}$ were also used. Concentration of LPF compounds was calculated by comparison of peak areas with those of known quantities of 5α-androstane. Quantification of HPF compounds was based on calibration curves ($r > 0.995$) using the area/$area_{IS}$ ratio versus the concentration of each reference compound. The concentration of LPF and HPF compounds is expressed as ng of individual compound per gram of dry sample (ng/gds).

2.5. Compound-specific isotope analysis of individual fatty acids

Carbon isotope analyses of individual *n*-fatty acids were done on a GC-C-IRMS system consisting on a Thermo Scientific Isotope Ratio Mass Spectrometer Delta V Advantage coupled to a GC Trace1310 through a Conflo IV interface with a temperature converter GC Isolink II, at the Archaeological Micromorphology and Biomarker Research Laboratory (University of La Laguna, Spain). Chromatography used a Trace Gold 5-MS (Thermo Scientific) capillary column (30 m length, 0.25 mm i.d. and 025 μm phase thickness), and Helium as carrier gas (1.5 mL/min). The temperature programme comprised a 2 min isothermal period at 70 °C, followed by an increase to 140 °C at a rate of 12 °C/min and held for 2 min. Finally, the temperature increased to 320 °C at a rate of 3 °C/min and held for 15 min. The combustion reactor temperature was maintained at 1000 °C. Samples were injected in splitless mode using a Programmed Temperature Vaporising (PTV) injector programmed with an evaporation step with the temperature increasing from 60 °C to 79 °C (held 30 s, rate 10 °C/min), followed by a transfer stage increasing to 325 °C (held 3 min, rate 10 °C/s) and a cleaning step with temperature increasing to 350 °C (held 3 min, rate 14 °C/S). The injection volume was 1 microlite.

A FAME standard mixture ($C_{14:0}$ methyl ester to $C_{20:0}$ ethyl ester, Arndt Schimmelmann Biogeochemical Laboratories, Indiana University) of known isotopic value was run prior to each batch of analyses to ensure that the combustion furnace and instrument were functioning correctly. The standard deviation of the standard fatty acid methyl esters mixture was better than or equal to ±0.5‰ for all analyses. Each sample was run in triplicate. Isotopic results are reported in the common "Delta" notation as ‰ relative to Vienna Pee Dee Belemnite (VPDB).

A correction was made to all the free fatty acid results for the isotopic signature of the introduced methyl groups using the mass balance equation (equation (1)) used by Goodman and Brenna (1992):

$$\delta^{13}C_{FA} = [((n+1)\delta^{13}C_{FAME}) - \delta^{13}C_{me}] / n \quad (1)$$

where $\delta^{13}C_{FA}$ is the corrected value for the free fatty acid, *n* is the number of carbon atoms in the unmethylated fatty acid, $\delta^{13}C_{FAME}$ is the value for the methylated fatty acid and $\delta^{13}C_{me}$ is the isotopic value of the methanol used for the methylation.

To account for the decrease in atmospheric $^{13}CO_2$ associated with the ^{13}C Suess effect, the modern $\delta^{13}C$ values are corrected by +1.9‰ to match archaeological values, assuming a preindustrial atmospheric $\delta^{13}C$ value of −6.4‰ (McCarroll and Loader, 2004) and the $\delta^{13}C_{atm}$ value at the time of sampling (−8.3‰) (Keeling et al., 2010).

2.6. Statistical analyses

Statistical analyses, one-way ANOVA (alpha level of 0.05) and confidence ellipses of a two-dimensional dataset, were performed on Microsoft Excel 365 and the Statistica software ver. 13. We used analysis of variance to compare isotopic signatures and determine differences between plant tissues, or between plant oils and animal fats. The one-way ANOVAs for $\delta^{13}C_{16:0}$ and $\delta^{13}C_{18:0}$ were done on i) a dataset with *Celtis australis* tissue samples ii) a dataset with angiosperm (*Celtis*) and gymnosperm (pine) tissue samples iii) a dataset with experimental hearth samples and iv) a dataset with C_3 tissues (leaves, wood, seeds …) and animal fat samples (terrestrial carnivores, herbivores, omnivores and marine carnivores). Datasets were performed using modern reference samples of C_3 leaves (this study and Chikaraishi et al., 2004a,b), C_3 wood (this study), seeds (this study, Steele et al., 2010; Recio et al., 2013, Lucquin et al., 2016, 2018) and animal fats (Evershed et al., 2002; Craig et al., 2011, 2012, 2013; Recio et al., 2013; Taché and Craig, 2015; Lucquin et al., 2016, 2018). The alpha value or significance level was 0.05. We calculated 95% confidence ellipses of $\delta^{13}C_{16:0}$ and $\delta^{13}C_{18:0}$ for i) anatomical parts of *Celtis australis* and for ii) C_3 plant oils and animal fats to test the variability of bivariate group means.

3. Results

3.1. Low/medium polarity fraction

Compounds identified in the experimental (laboratory heating sequence and open hearths) and archaeological samples (combustion sediments) contained biomarkers such as ketones, *n*-alkyl nitriles, *n*-alkyl aldehydes and fatty acid methyl esters (FAMEs), and are reported in SM 1. Saturated *n*-alkyl nitriles were detected from their mass spectrum which has a base peak at m/z 57, key ions at m/z 97 and 110.

3.1.1. Modern plant samples: laboratory heating sequence

In fresh and charred (150 °C) *Celtis* leaves we found trimethyl 2-pentadecanone (6.1 μg/gds), unsaturated short-chain FAMEs (*n*-$C_{16:0}$ and *n*-$C_{18:0}$) as well as long-chain FAMEs (*n*-$C_{24:0}$ to *n*-$C_{30:0}$) maximising at *n*-C_{26} (5.2–6.8 μg/gds). At 250 °C (1, 3 and 5 h) the length of the chain of FAMEs shorted up to *n*-$C_{22:0}$, maximising at *n*-$C_{16:0}$. After 3 and 5 h of charring at 250 °C and at 350 °C (1 h) the concentration of FAMEs and *n*-alkyl aldehydes decreased (*n*-$C_{16:0}$ $FAME_{max} = 5$ ng/gds) whereas a series of unsaturated *n*-alkyl nitriles appear in increasing concentration with increasing combustion time and temperature ranging from *n*-C_{16} to *n*-C_{24} and C_{max} at *n*-C_{16} (8.8 ng/gds at 250 °C − 3 h, 17.6 ng/gds at 250 °C − 5 h and 73.6 ng/gds at 350 °C − 1 h). At 450 °C only *n*-$C_{16:0}$ and *n*-$C_{18:0}$ FAMEs were found a very low concentration (3.9 and 3.3 ng/gds) (SM1 and Fig. 1).

Short-chain ketones (trimethyl 2-pentadecanone, heptadecan-2-one and nonadecan-2-one) and FAMEs ranging from *n*-$C_{16:0}$ to *n*-$C_{22:0}$ were found at an increasing concentration up to 150 °C in *Celtis* bark samples. At 250 °C, ketone concentrations decreased whereas *n*-alkyl aldehydes and FAMEs slightly increased (*n*-$C_{16:0}$ $FAME_{max} = 95.2$ ng/gds). At 350 °C, FAMEs drastically decreased (*n*-$C_{22:0}$ max = 4.9 ng/gds) as well as the aldehyde concentration; *n*-alkyl nitriles were detected (*n*-C_{22} max = 4.4 ng/gds). Lipid biomarkers were absent at 450 °C (SM1 and Fig. 1).

In xylem samples only FAMEs from *n*-$C_{16:0}$ to *n*-$C_{26:0}$ were found with *n*-$C_{16:0}$ as dominant. Similarly to leaf and bark samples, a higher concentration of *n*-$C_{16:0}$ FAME was found at 150 °C (39.5 ng/gds) and decreased with increasing combustion temperature (16.8 ng/gds at 350 °C) (SM1 and Fig. 1).

In fresh *Celtis* root samples *n*-$C_{16:0}$ FAME was detected (14.2 ng/

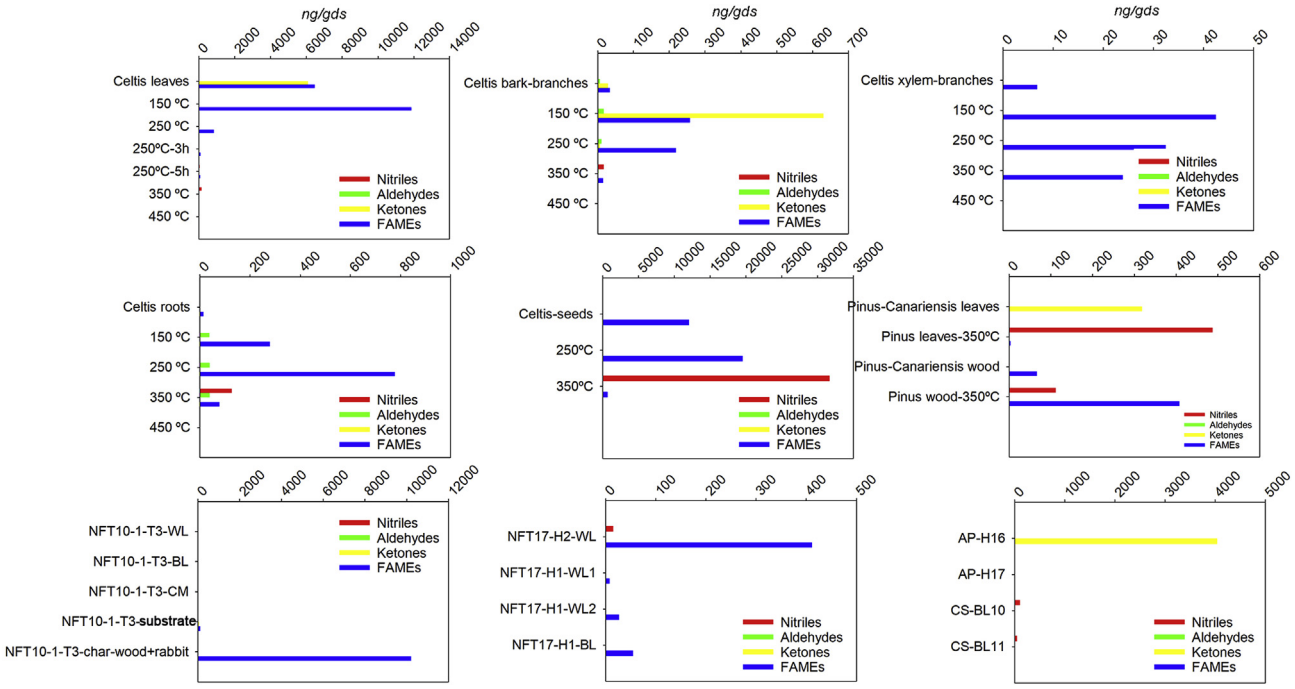

Fig. 1. Low and medium polarity compounds (ketones, *n*-alkyl aldehydes, *n*-alkyl nitriles, and fatty acid methyl esters) identified in the organic matter from laboratory-controlled heating experiments, open hearth experiments and El Salt, Abric del Pastor and Crvena Stijena hearth residues. Concentrations are expressed as ng of individual compound per gram of dry sample (ng/gds).

gds) and at 150 °C *n*-$C_{20:0}$ FAME (65.9 ng/gds) and *n*-$C_{21:0}$ FAME (153.2 ng/gds). FAMEs ranging from *n*-$C_{16:0}$ to *n*-$C_{22:0}$ and C_{max} at *n*-$C_{16:0}$ (436.0 ng/gds) and *n*-alkyl aldehydes were detected at 250 °C. At 350 °C, FAME concentrations decreased (*n*-$C_{16:0}$ = 21.0 ng/gds), *n*-alkyl aldehydes increased and *n*-alkyl nitriles ranging from *n*-C_{16} to *n*-C_{23} (*n*-C_{max} at 16 = 49.4 ng/gds) were detected (SM1 and Fig. 1).

Short-chain FAMEs (*n*-$C_{16:0}$ and *n*-$C_{18:0}$) were dominant in fresh and charred seeds and recorded higher concentrations than other tissues. *n*-Alkyl nitriles (*n*-C_{16}, *n*-C_{18} and oleanitrile) were detected at higher concentrations at 350 °C (SM1 and Fig. 1).

In fresh pine needles, we detected an asymmetric long-chain ketone (C_{29}-nonacosan-10-one = 318.3 ng/gds), and after a charring temperature of 350 °C *n*-alkyl nitriles ranging from *n*-C_{14} to *n*-C_{18} (*n*-C_{max} at 16 = 232.8 ng/gds). Fresh pine wood samples (bark and xylem included) shown high concentration of *n*-$C_{18:0}$ FAME (54.1 ng/gds) whereas in charred samples (350 °C) *n*-$C_{22:0}$ and *n*-$C_{24:0}$ FAMEs were also detected (*n*-$C_{16:0}$ was the dominant peak = 317.3 ng/ds) as well as *n*-C_{16} and *n*-C_{18} alkyl nitriles (71.8 and 40.2 ng/gds respectively) (SM1 and Fig. 1).

3.1.2. Experimental hearths

In the *Celtis* wood-rabbit hearth (NFT10-1-T3) we detected FAMEs ranging from *n*-$C_{16:0}$ to *n*-$C_{26:0}$ (Charcoal: C_{max} at *n*-C_{16} = 5.0 μg/gds). In the ash layer from the *Celtis*-wood hearth made over unvegetated sediment (NFT17-H2), *n*-C_{16} alkyl nitrile (14.6 ng/gds) and FAMEs ranging from *n*-$C_{16:0}$ to *n*-$C_{26:0}$ (C_{max} at *n*-$C_{16:0}$ = 273.5 ng/gds) were detected. However, in ash layers from the NTF17-H1 hearth (*Celtis* wood hearth over a *Celtis* leaf bedding) *n*−alkyl nitriles were not detected and only *n*-C_{16} FAME (26.2 ng/gds) and *n*-C_{18} FAME (7.3 ng/gds) were found in wood and leaf ashes but not in the wood ash sample. *n*-C_{16} FAME (54.1 ng/gds) was found in the charred-leaf sample (black layer) (SM1 and Fig. 1).

3.1.3. Archaeological samples

We did not find ketones, *n*-alkyl aldehydes, FAMEs and *n*-alkyl nitriles in any of the samples from El Salt (H50-BL-1, 2, 3, 4 and WL). In Abric del Pastor, oleanitrile (*n*-$C_{18:1}$; key ions m/z 122, 136), which is a nitrile derived from an 18-carbon unsaturated fatty acid was detected in AP-H17 (4.8 ng/gds) but not in H9, H13, H15, and H16. Two long-chain and symmetrical ketones: hentriacontan-16-one (95.4 ng/gds) and pentatriacontan-18-one (3943.2 ng/gds) were detected only in AP-H16. Black layers (CS-BL10 and 11) from Crvena Stijena recorded a series of long even *n*-alkyl nitriles from *n*-C_{24} to *n*-C_{28} (peaking at *n*-C_{28} = 23.1–50.2 ng/gds). In CS-BL8 and CS-WL6 these compounds were not detected (SM1 and Fig. 1).

3.2. High polarity fraction

3.2.1. Modern plant samples: laboratory heating sequence

In fresh and charred (150 °C) *Celtis* leaves we found unsaturated short-chain fatty acids (*n*-$C_{16:0}$ and *n*-$C_{18:0}$) as well as mid-chain fatty acids (*n*-$C_{20:0}$ to *n*-$C_{24:0}$) maximising at *n*-C_{18} (2.4 μg/gds) and at *n*-$C_{16:0}$ (8.6 μg/gds) (SM2). After 3 and 5 h of charring at 250 °C the concentration of FA decreased (long-chain FAs are present in higher concentrations), increased at 350 °C (C_{max} at *n*-$C_{26:0}$ = 9.1 μg/gds) and were absent at 450 °C. FAs ranging from *n*-$C_{16:0}$ to *n*-$C_{30:0}$ were found at a decreasing concentration up to 250 °C in *Celtis* bark samples (long-chain FAs were dominant maximising at *n*-$C_{26:0}$). In xylem samples only short-chain FAs (*n*-$C_{16:0}$ and *n*-$C_{18:0}$) were found with *n*-$C_{16:0}$ as dominant. Higher concentration of *n*-$C_{16:0}$ FA was found in fresh xylem samples (9.5 μg/gds) and decreased with increasing combustion temperature (4.2 μg/gds at 250 °C) (SM2).

In *Celtis* root samples short and mid-chain fatty acids ranging from *n*-$C_{16:0}$ to *n*-$C_{22:0}$ were detected (C_{max} at *n*-$C_{16:0}$=0.3 μ/gds). At 150 °C FA concentrations increased (C_{max} at *n*-$C_{16:0}$=0.8 μ/gds) (SM2).

Short-chain FAs were dominant in fresh (C_{max} at *n*-$C_{16:0}$=10.5 μ/

gds) and charred (C_{max} at n-$C_{18:0}$=1.6 μ/gds) seeds and recorded higher concentrations than other tissues (SM2).

n-$C_{16:0}$ and n-$C_{18:0}$ FAs were dominants in fresh and charred pine needles and wood (n-C_{max} at 16 = 5.4 and 3.3 μg/gds, respectively). At 350 °C, the concentration of short chain-FAs decreased (SM2).

3.2.2. Experimental hearths

In the *Celtis* wood-rabbit hearth (NFT10-1-T3) we detected FAs ranging from n-$C_{16:0}$ to n-$C_{22:0}$ (Charcoal: C_{max} at n-C_{16} = 0.2 μg/gds). Mid-chain FAs were found in the charcoal. In the ash layer from the *Celtis*-wood hearth made over unvegetated sediment (NFT17-H2), FAs ranging from n-$C_{16:0}$ to n-$C_{22:0}$ (C_{max} at n-$C_{22:0}$ = 0.3 μg/gds) were detected. However, in ash layers from the NTF17-H1 hearth only short-chain FAs (n-C_{16} = 0.4–0.8 μg/gds) and (n-C_{18} = 0.5 μg/gds) were found. Charred-leaf sample (black layer) reported higher short-chain FAs concentrations (n-C_{16} = 28.2 μg/gds) and (n-C_{18} = 24.1 μg/gds) (SM2).

3.2.3. Archaeological samples

Short-chain FAs (n-$C_{16:0}$ and n-$C_{18:0}$) were dominants in El Salt, Abric del Pastor and Crvena Stijena samples. However, in one sample from Crvena Stijena (CS-BL10), long-chain FAs were dominants (peaking at n-C_{28} = 0.3 μg/gds) (SM2).

3.3. Compound-specific stable carbon ($\delta^{13}C$) isotopic measurements of n-$C_{16:0}$ and n-$C_{18:0}$ fatty acids of the high polarity fraction

The results for modern (fresh and charred) plant tissues, experimental hearths and archaeological samples after correction for the isotopic signature of the introduced methyl groups are shown in Table 1.

3.3.1. Modern plant samples

The $C_{16:0}$ and $C_{18:0}$ fatty acid concentrations in leaves at 450 °C, bark (350 and 450 °C), roots (250–450 °C) and xylem (350 and 450 °C) were below the needed concentration to obtain reliable results and their $\delta^{13}C_{16:0}$ and $\delta^{13}C_{18:0}$ values could not be obtained. Fresh *Celtis* leaves had lower $\delta^{13}C_{16:0}$ and $\delta^{13}C_{18:0}$ values ($\delta^{13}C_{16:0}$ = −35.6‰ and $\delta^{13}C_{18:0}$ = −34.9‰) compared with bark ($\delta^{13}C_{16:0}$ = −34.9‰ and $\delta^{13}C_{18:0}$ = −33.6‰), root ($\delta^{13}C_{16:0}$ = −34.4‰ and $\delta^{13}C_{18:0}$ = −33.0‰) and xylem ($\delta^{13}C_{16:0}$ = −32.2‰ and $\delta^{13}C_{18:0}$ = −31.8‰) tissues. *Celtis* seeds had the highest $\delta^{13}C$ values of all the tissues ($\delta^{13}C_{16:0}$ = −30.3‰ and $\delta^{13}C_{18:0}$ = −31.2‰). $\delta^{13}C_{16:0}$ and $\delta^{13}C_{18:0}$ values in charred leaf and bark samples at 150 °C and 250 °C are similar than unheated tissues. However, xylem and root samples charred at 150 °C show higher $\delta^{13}C$ values. At 350 °C, there is a shift to more enriched $\delta^{13}C$ values in leaf samples (Table 1). $\delta^{13}C_{16:0}$ and $\delta^{13}C_{18:0}$ values in leaf samples after 3 h of charring at 250 °C were similar than those reported at 350 °C or also higher after 5 h of charring. In general, the $C_{18:0}$ fatty acid appears to be more enriched in ^{13}C than the $C_{16:0}$ fatty acid. Leaves and bark were depleted in ^{13}C relative to the signatures of roots and xylem (Table 2a). The ANOVA (alpha level of 0.05) performed on the $\delta^{13}C_{16:0}$ and $\delta^{13}C_{18:0}$ values in the different anatomical parts of *Celtis australis* tree showed that non-woody tissues (leaves and bark) and woody tissues (roots and xylem) were different ($\delta^{13}C_{16:0}$: F = 14.598, $F_{critical}$ = 4.667, p-value = 0.002; $\delta^{13}C_{18:0}$: F = 7.993, $F_{critical}$ = 4.667, p-value = 0.014).

$\delta^{13}C_{16:0}$ and $\delta^{13}C_{18:0}$ values of pine fresh needles were lower ($\delta^{13}C_{16:0}$ = −41.5‰ and $\delta^{13}C_{18:0}$ = −37.9‰) than after 1 h of charring at 350 °C ($\delta^{13}C_{16:0}$ = −33.6‰ and $\delta^{13}C_{18:0}$ = −30.2‰). $\delta^{13}C_{16:0}$ and $\delta^{13}C_{18:0}$ values were lower in fresh wood samples ($\delta^{13}C_{16:0}$ = −35.3‰ and $\delta^{13}C_{18:0}$ = −28.3‰) than on charred samples ($\delta^{13}C_{16:0}$ = −34.7‰ and $\delta^{13}C_{18:0}$ = −27.3‰) (Table 1). When we compared the leaves and wood of *Celtis* (angiosperms) and pine (gymnosperm), the isotopic values were not significantly different for any tissues (Table 2b).

3.3.2. Experimental hearths

In the NFT10-1-T3 hearth (*Celtis* wood-rabbit hearth) the charcoal and the ash layer are more enriched in ^{13}C than the brown layer and the substrate (Table 1). The fatty acids are enriched up to 4‰ in the charcoal and in the ash layer and by 2‰ in the brown layer. Concentrations of n-$C_{16:0}$ and n-$C_{18:0}$ fatty acids in the black layer were below the needed concentration to obtain reliable results and $\delta^{13}C$ values were not obtained. Ash layers from the wood hearths NFT17-H1 recorded similar $\delta^{13}C_{16:0}$ and $\delta^{13}C_{18:0}$ values ($\delta^{13}C_{16:0} \approx -31$‰ and $\delta^{13}C_{18:0} \approx -32$‰) but the ash layer-NFT17-H2 hearth showed higher $\delta^{13}C$ values ($\delta^{13}C_{18:0} \approx -26.5$‰). $\delta^{13}C_{16:0}$ and $\delta^{13}C_{18:0}$ values on black layer (H1) not differ from the ash layers (H1) ($\delta^{13}C_{16:0} \approx -32.1$‰ and $\delta^{13}C_{18:0} \approx -31.9$‰). When we compared $\delta^{13}C_{16:0}$ between experimental hearths using all the samples from the *Celtis* wood-hearth (plant oil contribution) and ash and charcoal samples from the *Celtis* wood-rabbit hearth (animal fat contribution), all values were different (ANOVA, F = 63.055, $F_{critical}$ = 7.709, p-value = 0.001). However, the $\delta^{13}C_{18:0}$ values for *Celtis* wood-hearth samples did not differ from the Celtis wood-rabbit hearth samples (ANOVA, F = 1.547, $F_{critical}$ = 7.709, p-value = 0.281) (Table 2c).

3.3.3. Archaeological samples

Black layers from El Salt (H50-BL1, 3 and 4) showed $\delta^{13}C_{16:0}$ values ranging from −33.6 to −32.1‰ and $\delta^{13}C_{18:0}$ values ranging from −32.5 to −29.2‰ (Table 1). The concentration of n-$C_{16:0}$ fatty acid in the black layer 2 (H50-BL2) and in the ash layer (H50-WL) was below the needed concentration to obtain reliable results and only $\delta^{13}C_{18:0}$ values were obtained in both samples (−31.8‰ and −33.5‰, respectively). Black layers samples from Abric del Pastor (H13 and H17) recorded $\delta^{13}C_{16:0}$ ranging from −33.6 to −30.9‰ and $\delta^{13}C_{18:0}$ values from −33.0 to −31.9‰ (Table 1). The concentration of n-$C_{16:0}$ fatty acid in H16 was below the needed concentration to obtain reliable results and only the $\delta^{13}C_{18:0}$ value was obtained ($\delta^{13}C_{18:0}$ = −31.5‰). Samples from Crvena Stijena (CS-BL10, CS-BL11 and CS-BL8) showed higher $\delta^{13}C_{16:0}$ and $\delta^{13}C_{18:0}$ values than El Salt and Abric del Pastor samples: $\delta^{13}C_{16:0}$ values ranged from −32.4 to −30.9‰ and $\delta^{13}C_{18:0}$ from −31.8 to −29.1‰ (Table 1). Fatty acid concentrations of n-$C_{16:0}$ and n-$C_{18:0}$ in CS-WL6 were below the needed concentration to obtain reliable results.

4. Discussion

4.1. n-Alkyl nitriles as a proxy for biomass burning and combustion temperature

A series of n-alkyl nitriles ranging from n-C_{16} to n-C_{24} with a strong even carbon number predominance and C_{max} = 16 were detected in *C. australis* (deciduous tree) leaf, bark, and root samples and in *P. canariensis* (conifer tree) leaf and wood samples charred to 350 °C (1 h). Similar findings have been reported by Simoneit et al., (2003), who detected nitriles after three days treatment of fatty acids with aqueous $(NH_4)HCO_3$ in confined vessels at an oven temperature of 300 °C (hydrous pyrolysis). Additionally, we identified n-alkyl nitriles in *Celtis* leaf samples charred at lower temperatures (250 °C) with increasing charring time (3 and 5 h). n-Alkyl nitriles were not detected after experimental heating to 450 °C. n-Alkyl nitriles ranging from n-C_{16} to n-C_{28} and C_{max} at 16 have been detected in birch tree smoke (a mixture of branches and leaves) by Oros and Simoneit (2001a). In kerogen pyrolysates after controlled heating at 310 °C (5–116 h) and 350 °C (5–100 h), the

Table 1
Compound-specific stable isotopes of n-$C_{16:0}$ and n-$C_{18:0}$ fatty acids of organic residues from laboratory-controlled heating experiments, open hearth experiments and El Salt, Abric del Pastor and Crvena Stijena hearths residues, with 1 standard deviation shown for samples with 3 replicates. The modern $\delta^{13}C$ values are normalised to the VPDB standard and corrected by +1.9‰ to match archaeological values. -: no data

		nC_{16} fatty acid (‰)	σ	nC_{18} fatty acid (‰)	σ	$\Delta = \delta^{13}C_{18:0}$-$\delta^{13}C_{16:0}$
Plant tissues	Celtis australis leaves	−35.6	±0.1	−34.9	±0.4	0.7
	Celtis leaves 150 °C	−36.6	±0.1	−35.0	±0.3	1.6
	Celtis leaves 250 °C	−35.8	±0.1	−34.1	±0.1	1.7
	Celtis leaves 250 °C	−34.9	±0.2	−34.7	±0.4	0.2
	Celtis leaves 250 °C-3h	−34.6	±0.3	−34.5	±0.5	0.1
	Celtis leaves 250 °C-5h	−32.6	±0.0	−26.4	±0.4	6.2
	Celtis leaves 350 °C	−34.9	±0.2	−34.7	±0.4	0.2
	Celtis australis bark	−34.9	±0.4	−33.6	±0.1	1.3
	Celtis bark 150 °C	−34.5	±0.5	−34.9	±0.5	−0.4
	Celtis bark 250 °C	−34.7	±0.3	−33.5	±0.3	1.3
	Celtis australis xylem	−32.2	±0.0	−31.8	±0.5	0.4
	Celtis xylem 150 °C	−31.8	±0.4	−28.8	±0.5	2.9
	Celtis xylem 250 °C	−33.1	±0.5	−27.1	±0.4	6.0
	Celtis australis roots	−34.4	±0.3	−33.0	±0.1	1.4
	Celtis roots 150 °C	−32.1	±0.3	−27.0	±0.3	5.1
	Celtis australis seeds	−30.3	±0.2	−31.2	±0.3	−0.9
	Celtis australis 250 °C	−34.0	±0.4	−37.1	±0.2	−3.1
	Pine canariensis leaves	−41.5	±0.4	−37.9	±0.3	3.5
	Pine leaves 350 °C	−33.6	±0.4	−30.2	±0.2	4.5
	Pine canariensis wood	−35.3	±0.0	−28.3	±0.1	7.0
	Pine wood 350 °C	−34.7	±0.0	−27.3	±0.5	7.4
Celtis-wood + rabbit hearth	NFT10-1-T3-WL	−29.4	±0.2	−28.6	±0.1	0.8
	NFT10-1-T3-CM	−30.9	±0.2	−28.0	±0.4	2.9
	NFT10-1-T3-substrate	−33.5	±0.2	−30.5	±0.2	3.0
	NFT10-1-T3-charcoal	−29.2	±0.3	−27.5	±0.3	1.7
Celtis-wood hearth	NFT17-H1-WL	−31.4	±0.4	−32.1	±0.3	−0.7
	NFT17-H1-WL	−31.6	±0.3	−32.3	±0.2	−0.8
	NFT17-H1-BL	−32.1	±0.0	−31.9	±0.1	0.1
	NFT17-H2-WL	−32.3	±0.1	−26.5	±0.4	5.8
El Salt	H50-WL	–	–	−33.5	±0.3	–
	H50-BL1	−33.5	±0.3	−31.3	±0.4	2.2
	H50-BL2	–	–	−31.8	±0.3	–
	H50-BL3	−33.6	±0.2	−29.2	±0.2	4.4
	H50-BL4	−32.1	±0.4	−32.5	±0.4	−0.4
Abric del Pastor	AP-H16	–	–	−31.5	±0.4	–
	AP-H13	−33.6	±0.2	−33.0	±0.4	0.6
	AP-H17	−30.9	±0.4	−31.9	±0.1	−1.0
Crvena Stijena	CS-BL10	−32.4	±0.4	−29.1	±0.4	3.2
	CS-BL11	−31.5	±0.4	−30.1	±0.2	1.4
	CS-BL8	−30.9	±0.4	−31.8	±0.5	−0.8

most intense n-alkyl nitrile peak was n-C_{16} (Ishiwatarii et al., 1992). In smoke from meat cooking experiments (charbroiling and frying of meat), two nitriles palmitonitrile and stearonitrile were identified (Rogge et al., 1991).

Whereas the highest n-alkyl nitrile concentrations were found in seed samples, n-alkyl nitriles were not detected in xylem samples. The absence of nitriles in *Celtis* xylem samples could suggest a low concentration of fatty acids to produce nitriles and absence of ammonia. Jambrina-Enríquez et al. (2018) reported an increase in fatty acid concentrations of charred leaf and bark *Celtis* tissue at 350 °C (93.8 and 24.7 μg/gds respectively) but lower concentrations in xylem samples (0.8 μg/gds). We calculated the total concentration of fatty acids in roots charred at 350 °C (1 h) and it was 0.5 μg/gds, but n-alkyl nitriles were detected in higher concentrations than in bark samples (SM2). This may be related to root absorption of nitrogen (NH_4^+ and NO_3^-) from the soil solution (Bloom et al., 2012). In deciduous species, N storage occurs in tissues such as roots and in the bark (Frak et al., 2002; Millard and Grelet, 2010). Simoneit et al. (2003) proposed that fatty acids react with ammonia during biomass burning to produce nitriles. The concentration of n-alkyl nitriles in *P. canariensis* leaf and wood samples were higher than in *C. australis* leaf and wood samples. This may be related to plant family effects (angiosperms vs. gymnosperms) on the biomarker composition and abundance. These observations should be examined for other species to determine if this is a common pattern.

n-Alkyl nitriles were not detected in samples from the wood and rabbit hearth, probably due to the higher combustion temperatures, since the temperature increased up to 740 °C on surface sediments and up to 418 °C at 2 cm below the surface. The piece of *Celtis* charcoal which showed good preservation of the bark reported FAMEs ranging from n-$C_{16:0}$ to n-$C_{26:0}$ ($C_{max} = 16$) and n-C_{16} and n-C_{17} ethyl esters. Due to the good preservation of the bark and based on our laboratory heating experiments, the temperature and combustion time was insufficient to produce n-alkyl nitriles. In the wood hearth over unvegetated sediment (NFT-17-H2) experiment, we detected hexadecanitrile in the ash layer (14.6 ng/gds) and FAMEs ranging from n-$C_{16:0}$ to n-$C_{26:0}$ (C_{max} at 16). However, n-C_{16} or n-C_{18} nitriles were not detected in the ash layers (wood + leaves or mostly leaves) from the wood hearth over vegetated sediment (NFT17-H1). Absence of nitriles may be attributed to the white layer from H2 containing more charcoal fragments in the ash than the white layer of H1, which preserved n-alkyl nitriles. These compounds have been detected in smoke particles from wildfires (Alves et al., 2011). These findings, as well as those previously reported by Simoneit et al. (2003), corroborate the potential of nitriles to be used as combustion biomarkers of smouldering conditions (<450 °C).

Table 2
Results of the one-way ANOVAs (alpha level of 0.05) for the comparison of the stable isotope values between plant oils and animal fats, using a) different anatomical parts of *Celtis australis* tree, b) angiosperm (*Celtis australis*) and gymnosperm (*Pinus canariensis*) tissue samples, c) experimental hearth samples and d) C_3 plant oils (leaves, wood, seeds …) and animal fat (terrestrial carnivores, herbivores, omnivores and marine carnivores) samples. Datasets were performed using modern reference samples of C_3 leaves (this study and Chikaraishi et al., 2004a,b), C_3 wood (this study), seeds (this study, Steele et al., 2010; Recio et al., 2013; Lucquin et al., 2016, 2018) and animal fats (Evershed et al., 2002; Craig et al., 2011, 2012, 2013; Recio et al., 2013; Taché and Craig, 2015; Lucquin et al., 2016, 2018).

		Sum of Squares	d.f.	Mean squares	F	p-value	F critical value
a) ANOVA of non-woody (leaf and bark, n = 10) and woody (xylem and root, n = 5) tissues of *Celtis australis*.							
C16:0	Inter-groups	15.987	1	15.987	14.598	0.002	4.667
	Intra-groups	14.237	13	1.095			
	Total	30.224	14				
C18:0	Inter-groups	55.76	1	55.76	7.993	0.014	4.667
	Intra-groups	90.693	13	6.976			
	Total	146.453	14				
b) ANOVA of leaves (*Celtis*, n = 7 and pine, n = 2) and wood (*Celtis* n = 6 and pine, n = 2) samples							
	Leaves	Sum of Squares	d.f.	Mean squares	F	p-value	F critical value
C16:0	Inter-groups	10.115	1	10.115	1.739	0.229	5.591
	Intra-groups	40.705	7	5.815			
	Total	50.82	8				
C18:0	Inter-groups	0.521	1	0.521	0.041	0.845	5.591
	Intra-groups	88.499	7	12.643			
	Total	89.020	8				
	Wood	Sum of Squares	d.f.	Mean squares	F	p-value	F critical value
C16:0	Inter-groups	3.227	1	3.227	2.079	0.199	5.987
	Intra-groups	9.313	6	1.552			
	Total	12.540	7				
C18:0	Inter-groups	4.950	1	4.950	4.723	0.073	5.987
	Intra-groups	6.288	6	1.048			
	Total	11.239	7				
c) ANOVA of experimental hearth samples (NFT17, n = 4 and NFT10, n = 2)							
		Sum of Squares	d.f.	Mean squares	F	p-value	F critical value
C16:0	Inter-groups	8.670	1	8.670	63.055	0.001	7.709
	Intra-groups	0.550	4	0.138			
	Total	9.220	5				
C18:0	Inter-groups	7.680	1	9.363	1.547	0.281	7.709
	Intra-groups	23.780	4	6.051			
	Total	31.460	5				
d) ANOVA of C_3 plant oils (C_3-leaves, n = 22; C_3-wood, n = 10; seeds, n = 12) and animal fats (terrestrial carnivores, n = 6; herbivores, n = 33; omnivores, n = 3, and marine carnivores, n = 28)							
		Sum of Squares	d.f.	Mean squares	F	p-value	F critical value
C16:0	Inter-groups	3556.047	6	592.675	119.458	0.000	2.184
	Intra-groups	530.865	107	4.961			
	Total	4086.912	113				
C18:0	Inter-groups	3121.858	6	520.310	78.128	0.000	2.184
	Intra-groups	712.589	107	6.660			
	Total	3834.447	113				

4.2. Effects of combustion on $nC_{16:0}$ and $nC_{18:0}$ fatty acids and potential sources in modern references

Celtis leaves (fresh and charred up to 350 °C), bark-branches (fresh and charred up to 250 °C, and roots (fresh) plot closely together on the $\Delta^{13}C$ plot ($\delta^{13}C_{18:0}$-$\delta^{13}C_{16:0}$) (Fig. 2a). Xylem branches (fresh and charred up to 250 °C) and roots (charred at 150 °C) are plotted in a different area ($\delta^{13}C_{16:0}$ values are more enriched in ^{13}C) (Fig. 2a). The $\delta^{13}C_{18:0}$-$\delta^{13}C_{16:0}$ plot shows that all the leaf and bark oils lie in the same group and xylem oils in another group (all data are plotted with 95% confidence ellipse) (Fig. 3a) (ANOVA, F = 14.598, F critical = 4.667, p-value = 0.002, Table 2a). Possibly, leaf and bark tissue plots in a different area than xylem tissue because cuticular wax composition varies widely by tissue, organ or across stages of development within an individual organism (Post-Beittenmiller, 1996). Moreover, *n*-alkanes from fresh stems and xylems are enriched in ^{13}C relative to leaves due to internal biosynthetic fractionation during C transport and fixation (Hobbie and Werner, 2004; Wiesenberg et al., 2004; Jambrina-Enríquez et al., 2018).

The $\delta^{13}C$ value for the uncharred *Celtis* seed is plotted in the area generally accepted for ruminant adipose (Dudd et al., 1999) (Fig. 2a). Similarly, other seed oils (almond, argan, olive, sesame, walnut and moringa oils, Steele et al., 2010) had higher $\delta^{13}C$ values, lying within the range of values generally accepted for animal (ruminant and pork) fat. On the other hand, acorn (Recio et al., 2013; Lucquin et al., 2018) and chestnut (Lucquin et al., 2018) oils have shown to be isotopically depleted in ^{13}C plotting far from the animal fat area.

Examination of the $\delta^{13}C$ values of *Celtis* leaves (Fig. 3a) with combustion temperature indicates that there is a shift to higher $\delta^{13}C_{16:0}$ values at 350 °C, and in general the longer-chained fatty acid (n-$C_{18:0}$) appears in all the tissue types to be more enriched in ^{13}C than the shorter-chained fatty acid (n-$C_{16:0}$). This relationship was observed in aerosol samples of cedar trees (eucalyptus, C_3 vegetation, angiosperm) collected under smouldering (150 °C) and flaming (500 °C) conditions; the fatty acids obtained from burned leaves showed an isotopic enrichment of up to 5‰ relative to the unburned leaves and $C_{18:0}$ appears to be more enriched in ^{13}C than $C_{16:0}$ fatty acids (Ballentine et al., 1998). As temperature increased, $\delta^{13}C_{16:0}$ values in leaves were depleted in ^{13}C at 150 °C and enriched in ^{13}C up to 350 °C, whereas in xylem samples $\delta^{13}C_{18:0}$ values were enriched in carbon-13. n-$C_{16:0}$ and n-$C_{18:0}$ fatty acids produced in charred needles at 350 °C are enriched by 8‰ in ^{13}C relative to those from fresh needles, whereas charred branches are enriched by in 1‰ ^{13}C (Fig. 3a).

Interestingly, a comparison of $\delta^{13}C$ values of fatty acids extracted from the white layer in the experimental *Celtis* wood-rabbit hearth

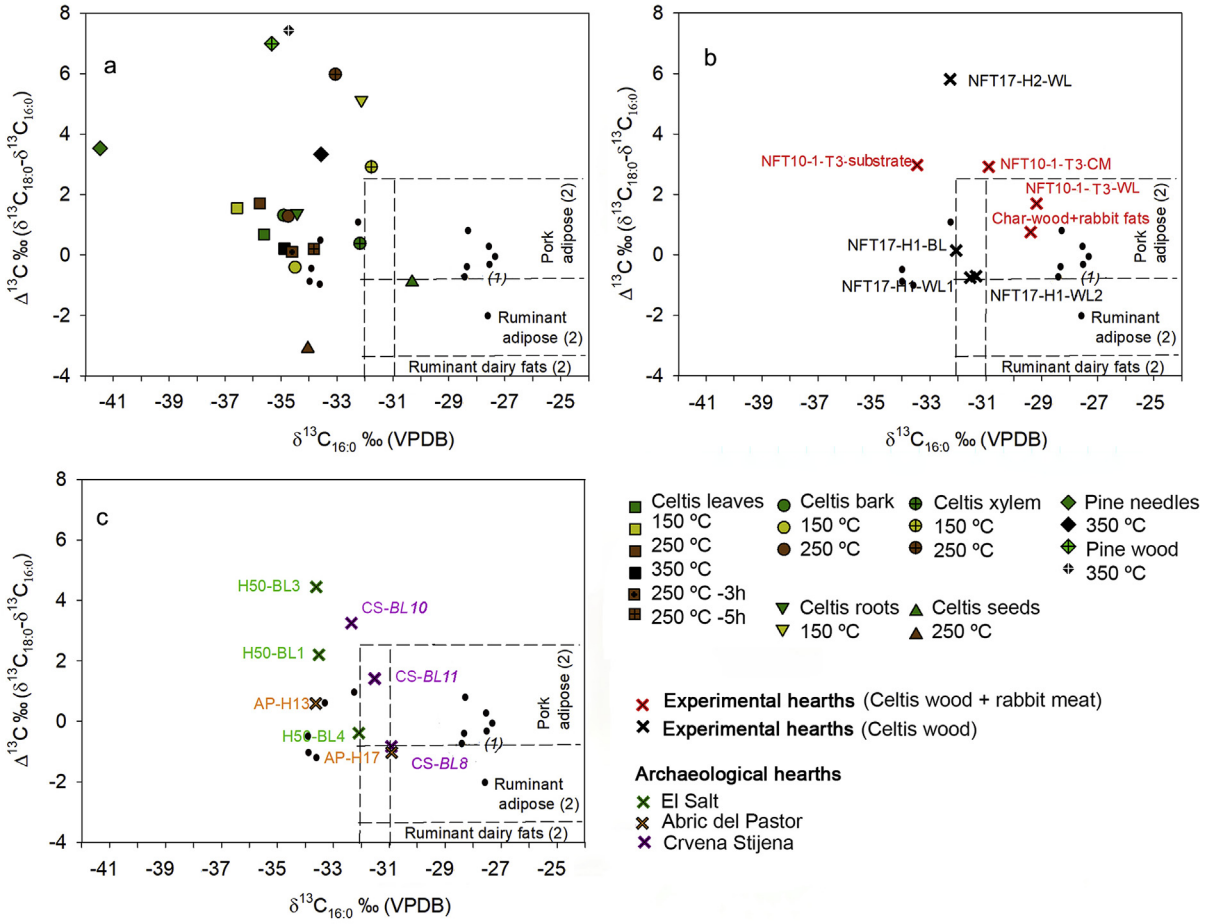

Fig. 2. Plots of $\Delta^{13}C$ against $\delta^{13}C_{16:0}$ for a) laboratory-controlled heating experiments, b) open hearth experiments, c) El Salt, Abric del Pastor, and Crvena Stijena hearth residues and comparison of modern plant oil reference samples from Steele et al. (2010), Recio et al. (2013), Lucquin et al. (2016) (1: black dots) and modern animal reference samples from Dudd et al. (1999) (2).

(NFT10-1-T3) and the white layers from *Celtis* wood hearths (H2 and H1) clearly demonstrate a different origin for these lipids (ANOVA, $F = 63.055$, $F_{critical} = 7.709$, p-value $= 0.001$) (Figs. 2b and 3b). The white layer (NFT10-1-T3) and the piece of *Celtis* charcoal strongly supports an animal fat contribution, as they plot close to the reference values of animal fats and are enriched in ^{13}C ($\delta^{13}C_{16:0} = -29‰$), whilst the fatty acids from the other white layers are derived from plant oils (*Celtis* wood and leaves) ($\delta^{13}C_{16:0} = -32‰$). Stable carbon isotope analysis of the brown ($\delta^{13}C_{16:0} = -30.9‰$ and $\delta^{13}C_{18:0} = -28.0‰$) and natural substrate layers in NFT10-1-T3 ($\delta^{13}C_{16:0} = -33.5‰$ and $\delta^{13}C_{18:0} = -30.5‰$) produced much lighter values than the samples from the white layer ($\delta^{13}C_{16:0} = -29.4‰$ and $\delta^{13}C_{18:0} = -28.6‰$) suggesting a decreasing contribution and preservation of animal fats (brown layer, barely affected by the overlying combustion) and a 'non-animal' component (natural substrate beneath the hearth and unaffected by it) (Fig. 2b). Charcoal fragments and white layers with good preservation and contribution of animal fat are isotopically enriched in ^{13}C (~4‰) compared to white layers and sediment free of animal fat. This finding agrees with the study reported by Recio et al. (2013) showing an enrichment of ca. ~5 in ^{13}C in fat from pigs feeding on winter acorns and grass compared to acorn oils (cork-oak acorns).

$\delta^{13}C_{16:0}$ and $\delta^{13}C_{18:0}$ values from C_3 leaves and C_3 wood (this study) and modern reference samples previously published by Chikaraishi et al. (2004a,b) (C_3 leaves) and by Craig et al. (2011, 2012, 2013); Taché and Craig (2015); Lucquin et al. (2016, 2018) (animal fats) were plotted with 95% confidence ellipses and experimental hearth samples were plotted. We also used variance analysis (one-way ANOVA) to investigate differences between the main groups (C_3-leaf oils, C_3-wood oils, and fats from terrestrial carnivores, herbivores, omnivores and marine carnivores). The differences in the isotopic values of these groups were significantly pronounced for $\delta^{13}C_{16:0}$ (ANOVA, $F = 119.458$, $F_{critical} = 2.184$, p-value $= 0.000$) and for $\delta^{13}C_{18:0}$ (ANOVA, $F = 78.128$, $F_{critical} = 2.184$, p-value $= 0.000$, Table 2d). Stable isotope signatures showed that the hearth experimental samples with animal fat contribution (ashes: NFT10-1-T3-WL and charcoals: char-wood + rabbit fats) plot in the area of animal fats, whereas samples without animal fat contribution (NFT10-1-T3-CM and substrate, NFT17-H1 and H2) plot close to the C_3 wood area (Fig. 4b).

Isotopic variations are detected among the white layers from the two wood-hearths H1 and H2. *n*-$C_{18:0}$ fatty acid in the white layer from the wood hearth (H2, only wood as fuel and on unvegetated sediment) is enriched by 6‰ in ^{13}C relative to the white layer from the *Celtis* wood hearth (leaves and wood) over vegetated sediment (H1) (Fig. 3b). In all likelihood, the fatty acids in WL- H1 are derived from a mixture of plant tissues more influenced by leaf oils. Stable isotope analysis of modern *Celtis* tissues shows that the $\delta^{13}C$ values of *n*-$C_{16:0}$ and *n*-$C_{18:0}$ fatty acids are lighter in leaf tissues (NFT10-H1) compared to xylem tissue (NFT10-H2). Comparison with the plant oil and animal fat areas (95% confidence ellipses, Fig. 4), H2

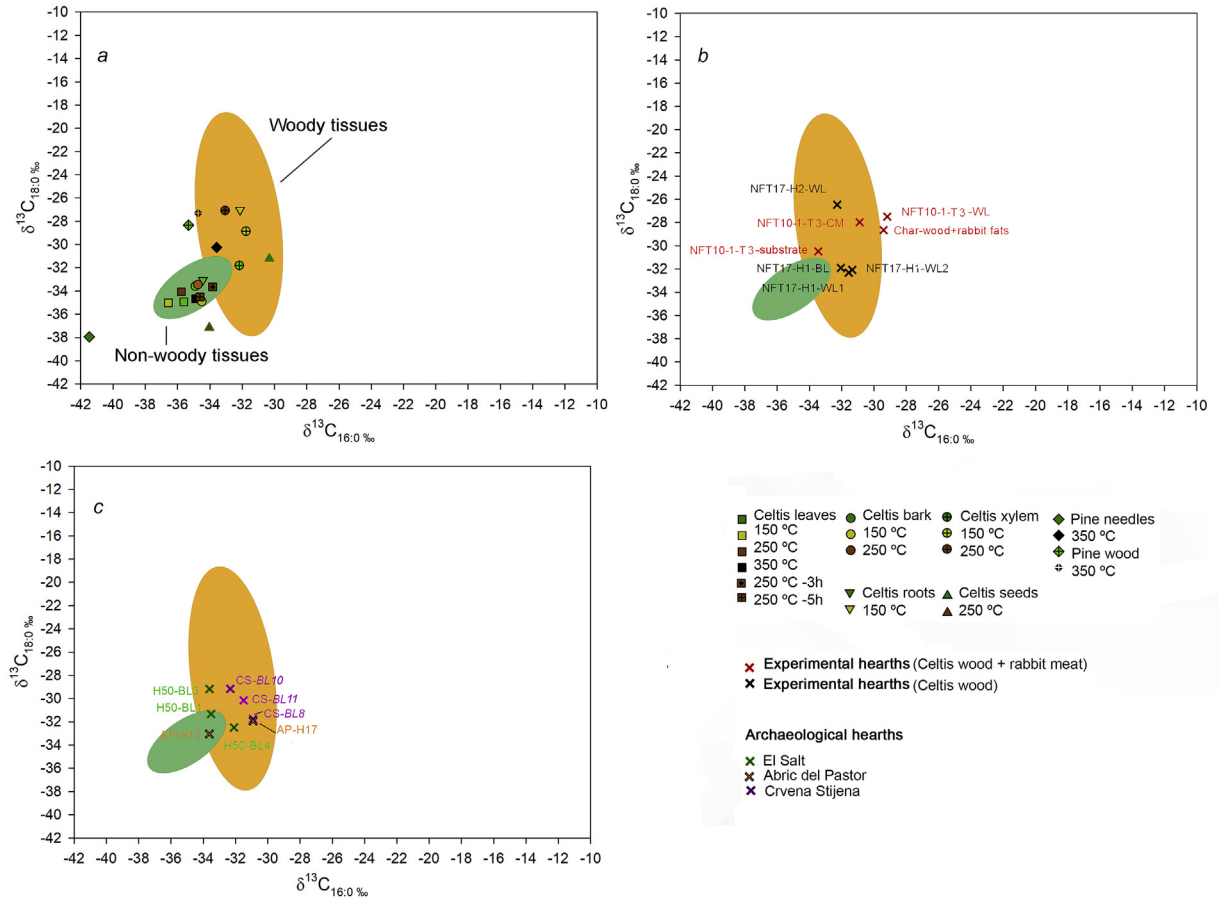

Fig. 3. $\delta^{13}C_{16:0}$ and $\delta^{13}C_{18:0}$ values of organic residues from a) laboratory-controlled heating experiments, b) open hearth experiments, c) El Salt, Abric del Pastor, and Crvena Stijena hearth residues. Modern references were adjusted for the addition of the post-industrial carbon effect and woody (roots and xylem) and non-woody (bark and leaves) Celtis tissues were plotted with 95% confidence ellipses.

and H1 plot close to the area of C_3 woody tissues (Fig. 4b). Considering isotopic enrichment increasing combustion temperature and the different isotopic signature of bark and xylem tissues, the extension or distribution of the C_3 woody area (woody tissues such as roots are also included) could be affected. More modern fresh and charred woody reference samples (driftwood, fresh-with bark, dead-xylem), should be included in future work.

4.3. Archaeological evidence

To compare reference and archaeological data, $\delta^{13}C$ values of experimental samples (including references previously published by Evershed et al., 2002; Chikaraishi et al., 2004a,b; Craig et al., 2011, 2012, 2013; Recio et al., 2013; Taché and Craig, 2015; Lucquin et al., 2016, 2018) were adjusted for the addition (1.9‰) of effects from post-industrial carbon (Figs. 2c and 3c). All data in Fig. 4 are plotted with 95% confidence ellipses.

Black layers from El Salt (H50-BL-1, 3 and 4) lie within the range of values for xylem samples and not in the area considered to represent ruminant or pork adipose (Figs. 2c and 3c). H50-BL4 and NFT17-H1-BL plot closely together on the plot of $\delta^{13}C_{16:0}$ and $\delta^{13}C_{18:0}$, and supports a mixture of plant tissue more influenced by leaf oils, as they plot close to the black layer of our experimental wood-hearth on vegetated sediment (Fig. 4). In contrast, H50-BL3 and H50-BL1 are more enriched in ^{13}C (high $\delta^{13}C_{18:0}$ values) and are therefore likely to derive from a woody source, more evident in H50-BL3 (Fig. 4). Comparison with our laboratory-controlled heating experiments, H50-BL3 is more enriched in ^{13}C (higher $\delta^{13}C_{18:0}$ values) than H50-BL1 and plot close to xylem samples charred at 150 °C and 250 °C, respectively (Figs. 2 and 3). We did not find ketones, *n*-alkyl aldehydes, and *n*-alkyl nitriles in any of the samples from El Salt (H50-BL-1, 2, 3, 4 and WL). Combustion temperatures below 350 °C could explain the absence of *n*-alkyl nitriles. Anthracological studies from the corresponding stratigraphic unit yielded predominant *Pinus nigra-sylvestris* (71–82%) followed by Acer sp. (20-7%) (Vidal-Matutano et al., 2018). Biomarker analysis in sediment samples from H50 (Leierer et al., 2019) reported that the absence of diterpenoids and their derived, along with presence of triterpenoids in BLs are evidence of an angiosperms forest (trees and shrubs) in the surrounding area, whereas conifer wood was used as fuel (possibly collected off-site). This is in agreement with the BLs representing the charred vegetated surface under the hearths, not fuel residues. Nonacosan-10-one (29-carbon ketone), a specific biomarker from burning conifers, was detected in our pine samples (350 °C) and in smoke particulate matter from other conifers (wood, bark, needles, and cones) subjected to controlled burning (Oros and Simoneit 2001b), probably under smouldering conditions (<300 °C), but no in BLs from H50. On the other hand, short-chain ketones have been reported in biomass burning (branches and leaves) of deciduous trees including maple tree (Cmax at 19) (Oros and Simoneit, 2001a) as well as in conifers trees (Oros and Simoneit 2001b) but no in BLs from H50. In our laboratory heating sequence, short-chain ketones were detected on fresh and charred (up to 250 °C) *Celtis* bark samples and in fresh *Celtis*

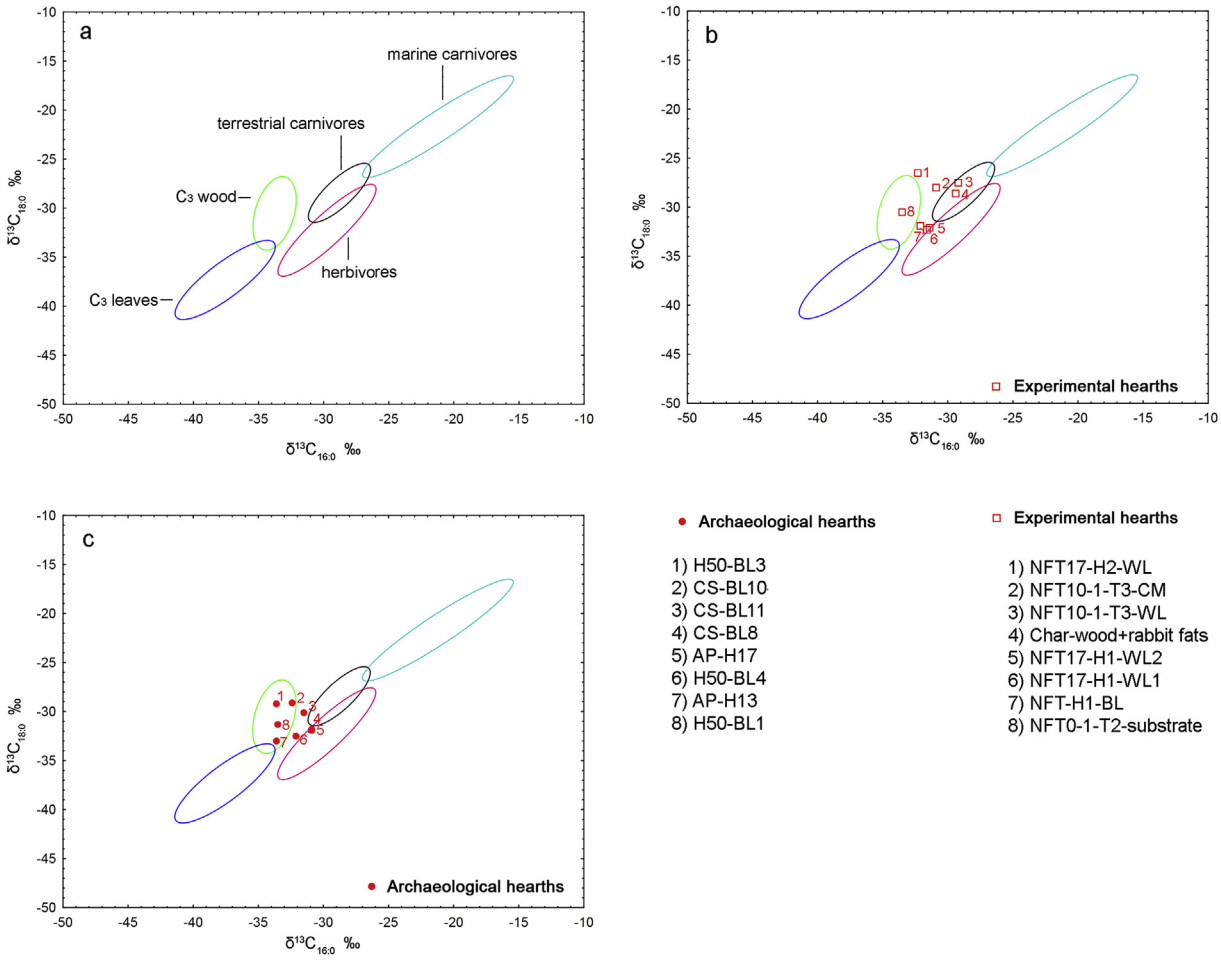

Fig. 4. Plots of the $\delta^{13}C_{16:0}$ and $\delta^{13}C_{18:0}$ values of organic residues from open hearth experiments (b) and El Salt, Abric del Pastor and Crvena Stijena hearth residues (c). These are compared with modern reference samples from C_3 leaves, C_3 wood, terrestrial carnivores, herbivores and terrestrial carnivores (Evershed et al., 2002; Chikaraishi et al., 2004a,b; Craig et al., 2011, 2012, 2013; Taché and Craig, 2015; Lucquin et al., 2016) and plotted as 95% confidence ellipses.

leaves, but not in xylem tissue. Taking into account that ketones were not detected in our xylem samples and that the $\delta^{13}C$ values of *n*-$C_{16:0}$ and *n*-$C_{18:0}$ fatty acids in our BL-3 are close to the xylem samples, we can assume a plausible contribution of lipids to the sediment from mostly bark-free wood.

In Abric del Pastor, H17 lies relatively close to the $\delta^{13}C_{18:0}$ *vs.* $\delta^{13}C_{16:0}$ area usually considered to represent terrestrial animal fats (Fig. 4c) or in the area of *Celtis* wood oils (Fig. 3c), whereas H13 plots close to leaf oil contributions (Fig. 3c). In H17 we found oleanitrile. Potential sources of alkyl nitriles include biomass burning (Oros and Simoneit, 2001a; Simoneit et al., 2003), cooking byproducts (Rogge et al., 1991; Simoneit et al., 2003) or contamination from plastic (Grosjean and Logan, 2007). In this case, *n*-$C_{18:1}$ as well as *n*-$C_{18:0}$ are the most abundant fatty acids, and the presence of oleamide (9-octadecenamide) detected in the derivatised (80 °C, 1 h) fraction eluted with 3 mL DCM/EtOAc (1:1, v:v) with the addition of 100 μL of bis-(trimethylsilyl) trifluoroacetamide (BSTFA) and 100 μL of pyridine, suggests that oleanitrile formed from the dehydration of the corresponding amide. Oleamide and other short-chain amides (*n*-C_{16} and *n*-C_{18}) are apparently strongly correlated with animal sources (Wang et al., 2017) and have been detected in archaeological sediments dating to 5 ka BP (Wang et al., 2017). These findings and the evidence that H17 was the sole hearth with a dense black layer and presence of microscopic char suggest plausible animal fat contribution. Although in H13 there are burnt materials such as bone and charcoal, the $\delta^{13}C_{16:0}$ and $\delta^{13}C_{18:0}$ values from the organic matter preserved in its sediment supports a leaf oil contribution and low preservation of animal fat (Fig. 4). In relation to burning practices, long-chain ketones as detected in H16, have been found in smoke particles from biomass burning (Abas and Simoneit, 1996) as well as in experimental bone-fire studies (Lejay et al., 2016; Buonasera et al., 2019).

In Crvena Stijena, not all the samples contained sufficient concentration of *n*-$C_{16:0}$ and *n*-$C_{18:0}$ as to provide reliable $\delta^{13}C$ values. CS-BL8 (a black layer overlain by a white layer) and CS-BL10, CS-BL11 (dense black lens with a greasy texture), contained sufficiently high *n*-$C_{16:0}$ and *n*-$C_{18:0}$ concentrations. Combined $\delta^{13}C_{16:0}$ and $\delta^{13}C_{18:0}$ values showed that these are distributed close to plant groups (*Celtis* branches-xylem charred below 350 °C) and the experimental *Celtis* wood hearth on a bed of *Celtis* leaves (Figs. 2c and 3c). *Celtis* is a potential source of organic matter in Palaeolithic sites from Mediterranean area (Hockett and Haws, 2002) and is currently present at the site and its surroundings. It interesting to note that CS-BL8 lies relatively close to the $\delta^{13}C_{16:0}$ and $\delta^{13}C_{18:0}$ area usually considered to terrestrial animal fats (Fig. 4c), suggesting a plausible animal fat contribution and good animal fat preservation whereas CS-BL10 and CS-BL11 fits a plant origin or low preservation of animal fat (Fig. 4c). Long-chain saturated nitriles (*n*-C_{24}–*n*-C_{28}), with a strong even carbon number predominance and $C_{max} = 28$ were identified in CS-BL10 and CS-BL11 with

concentrations from 14.2 to 50.2 ng/gds and from 8.2 to 23.2 ng/gds respectively. However, nitriles were not detected in CS-BL8 and in CS-WL6. A series of long-chain nitriles ranging from n-C_{25} to n-C_{34}, with a strong even carbon number predominance and maximising at 30 was reported in aerosol samples collected during a severe forest fire in Kuala Lumpur (Abas and Simoneit, 1996). Taking into account our indoor and outdoor experiments, combustion above 250 °C, as well as animal fat contribution, enriches $\delta^{13}C$ values. Given that nitriles are detected at combustion temperatures between 300 and 350 °C (our data and data from Simoneit et al., 2003) and their absence in CS-BL8, the fatty acids of this black layer seem to be enriched in ^{13}C by the contribution of animal fats. On the other hand, the $\delta^{13}C$ values of fatty acids and the presence of long-chained nitriles in CS-BL10 and CS-BL11 could imply combustion of plant tissues at temperatures around 300–350 °C.

5. Conclusions

Molecular and isotopic approaches offer the chance to identify organic burnt constituents of archaeological combustion structures, including animal and plant components to infer past fire-related activities (cooking practices or biomass burning).

Here we presented results from laboratory heating experiments on different anatomical parts of the *Celtis australis* tree (leaves, roots, seeds and branches-bark and xylem) and *Pinus canariensis* tree (needles and branches), as well as from open experimental hearths using *Celtis* wood (some of them with meat contribution) to identify its molecular (*n*-alkyl nitriles) and isotopic ($\delta^{13}C$-fatty acids) fingerprints and thus discern among different plant-tissue types, distinguish plant *vs.* animal contributions and approach combustion temperatures. We analysed sediment samples from ancient (Palaeolithic) archaeological structures to determine whether charred organic remains could be identified as plant or a mixture of plant and animal components comparing their isotope signatures with modern references.

The results showed that $\delta^{13}C$-fatty acid values of leaves (fresh and charred) are sufficiently different from those reported in wood and allow the distinction between fuel (wood) and the underlying soil substrate (mostly leaves) in the black layers of combustion structures. Also, the isotopic signatures from our hearth experiments showed that organic residues with animal fat contributions were enriched in ^{13}C ($\approx$4‰) compared to plant residues. From our experiments, it appears that organic residues preserved in archaeological combustion structures with depleted $\delta^{13}C_{16:0}$ values ($\delta^{13}C_{16:0} < -31$‰) could indicate biomass burning and low contribution and preservation of terrestrial animal fat. However, seeds can plot on the plant oil areas as well as on the animal (terrestrial) fat area. More modern wood reference samples (driftwood, fresh-with bark, dead-xylem and charred), as well as open hearth experiments combining wood and animal fats, should be included in future work to compile a complete database.

With respect to molecular fingerprints and combustion temperatures, a series of *n*-alkyl nitriles was detected in the reference samples at a temperature of 350 °C (1 h of combustion) and 250 °C (3–5 h of combustion) and identified in the archaeological samples. Our findings corroborate that *n*-alkyl nitriles and *n*-alkyl amides can be preserved in Pleistocene sediments and hold potential as combustion temperature biomarkers as well as to determine sources of organic matter.

Acknowledgements

This research was supported by the ERC Consolidator Grant project PALEOCHAR – 648871. The NFT10-1 experimental hearth was made with funding from a Leakey Foundation General Grant. Excavations and archaeological investigation at El Salt and Abric del Pastor sites were funded by Spanish Ministry of Science, Innovation and Universities Projects HAR2008-06117/HIST and HAR2015-68321-P and the Archaeological Museum of Alcoy and the Government of Valencia Cultural Heritage Department. Excavation and archaeological investigations at Crvena Stijena are funded by USA National Science Foundation Grant 1758285. We would like to thank two anonymous reviewers for their thoughtful and constructive comments. The authors thank Gil Tostevin, Gilliane Monnier, Nikola Borovinić, Mile Baković, Bertila Galván and Cristo Hernández, responsible for the archaeological research that enabled sample collection.

Appendix A. Supplementary data

Supplementary data to this article can be found online at https://doi.org/10.1016/j.quascirev.2019.105899.

References

Abas, M.R.B., Simoneit, B.R.T., 1996. Composition of extractable organic matter or air particles from Malaysia: initial study. Atmos. Environ. 30 (15), 2779–2793. https://doi.org/10.1016/1352-2310(95)00336-3.

Akazawa, T., 1987. The ecology of the middle paleolithic occupation at Douara Cave, Syria. In: Suzuki, H., Takai, F. (Eds.), Bulletin of the University Museum, University of Tokyo, vol. 29, p. 29012.

Allué, E., Cáceres, I., Expósito, I., Canals, A., Rodríguez, A., Rosell, J., Bermúdez de Castro, J.M., Carbonell, E., 2015. Celtis remains from the lower Pleistocene of gran Dolina, Atapuerca (Burgos, Spain). J. Archaeol. Sci. 53, 570–577. https://doi.org/10.1016/j.jas.2014.11.016.

Alves, C.A., Vicente, A., Monteiro, C., Gonçalves, C., Evtyugina, M., Pio, C., 2011. Emission of trace gases and organic components in smoke particles from a wildfire in a mixed-evergreen forest in Portugal. Sci. Total Environ. 409 (8), 1466–1475. https://doi.org/10.1016/j.scitotenv.2010.12.025.

Ballentine, D.C., Macko, S.A., Turekian, V.G., 1998. Variability of stable carbon isotopic compositions in individual fatty acids from combustion of C4 and C3 plants: implications for biomass burning. Chem. Geol. 152 (1–2), 151–161. https://doi.org/10.1016/S0009-2541(98)00103-X.

Beaufort, L., de Garidel-Thoron, T., Linsley, B., Oppo, D., Buchet, N., 2003. Biomass burning and oceanic primary production estimates in the Sulu Sea area over the last 380 kyr and the East Asian monsoon dynamics. Mar. Geol. 201, 53–65. https://doi.org/10.1016/S0025-3227(03)00208-1.

Bloom, A.J., Randall, L., Taylor, A.R., Silk, W.K., 2012. Deposition of ammonium and nitrate in the roots of maize seedlings supplied with different nitrogen salts. J. Exp. Bot. 63–5, 1997–2006. https://doi.org/10.1093/jxb/err410.

Buonasera, T., Herrera-Herrera, A., Mallol, C., 2019. Experimentally derived sedimentary, molecular, and isotopic characteristics of bone-fueled hearths. J. Archaeol. Method Theory. https://doi.org/10.1007/s10816-019-09411-3.

Buonasera, T.Y., Tremayne, A.H., Darwent, C.M., Eerkens, J.W., Mason, O.K., 2015. Lipid biomarkers and compound specific $\delta^{13}C$ analysis indicate early development of a dual-economic system for the Arctic Small Tool tradition in northern Alaska. J. Archaeol. Sci. 61, 129–138. https://doi.org/10.1016/j.jas.2015.05.011.

Chikaraishi, Y., Naraoka, H., Poulson, S.R., 2004a. Carbon and hydrogen isotopic fractionation during lipid biosynthesis in a higher plant (Cryptomeria japonica). Phytochemistry 65, 323–330. https://doi.org/10.1016/j.phytochem.2003.12.003.

Chikaraishi, Y., Naraoka, H., Poulson, S.R., 2004b. Hydrogen and carbon isotopic fractionations of lipid biosynthesis among terrestrial (C3, C4 and CAM) and aquatic plants. Phytochemistry 65 (10), 1369–1381. https://doi.org/10.1016/j.phytochem.2004.03.036.

Choy, K., Potter, B.A., McKinney, H.J., Reuther, J.D., Wang, S.W., Wooller, M.J., 2016. Chemical profiling of ancient hearths reveals recurrent salmon use in Ice Age Beringia. Proc. Natl. Acad. Sci. 113, 9757–9762. https://doi.org/10.1073/pnas.1606219113.

Clark, J.D., Harris, J.W.K., 1985. Fire and its roles in early hominid lifeways. Afr. Archaeol. Rev. 3, 3–27.

Costa, M., Morla, C., Sainz, H., 1998. Los Bosques Ibéricos. Editorial Planeta, Barcelona.

Collins, J.A., Andrez, S., Carr, A.S., Schefuß, E., Boom, A., Sealy, J., 2017. Investigation of organic matter and biomarkers from Diepkloof Rock Shelter, South Africa: insights into middle stone age site usage and palaeoclimate. J. Archaeol. Sci. 85, 51–65. https://doi.org/10.1016/j.jas.2017.06.011.

Craig, O.E., Forster, M., Andersen, S.H., Koch, E., Crombe, P., Milner, N.J., Stern, B., Bailey, G.N., Heron, C.P., 2007. Molecular and isotopic demonstration of the processing of aquatic products in northern European prehistoric pottery. Archaeometry 49, 135–152. https://doi.org/10.1111/j.1475-4754.2007.00292.x.

Craig, O.E., Steele, V.J., Fischer, A., Hartz, S., Andersen, S.H., Donohoe, P., Glykoug, A., Saul, H., Jones, D.M., Koch, E., Heron, C.P., 2011. Ancient lipids reveal continuity in culinary practices across the transition to agriculture in Northern Europe. Proc. Natl. Acad. Sci. 108, 17910–17915. https://doi.org/10.1073/pnas.

1107202108.
Craig, O.E., Allen, R.B., Thompson, A., Stevens, R.E., Steele, V.J., Heron, C.P., 2012. Distinguishing wild ruminant lipids by gas chromatography/combustion/isotope ratio mass spectrometry. Rapid Commun. Mass Spectrom. 26, 2359–2364. https://doi.org/10.1002/rcm.6349.
Craig, O.E., Saul, H., Lucquin, A., Nishida, Y., Taché, K., Clarkes, L., Thompson, A., Altoft, D.T., Uchiyama, J., Ajimoto, M., Gibbs, K., Isaksson, S., Heron, C.P., Jordan, P., 2013. Earliest evidence for pottery use. Nature 496, 351–354. https://doi.org/10.1038/nature12109.
Daniau, A.L., d'Errico, F., Sánchez Goñi, M.F., 2010. Testing the hypothesis of fire use for ecosystem management by neanderthal and upper palaeolithic modern human populations. PLoS One 5 (2), e9157. https://doi.org/10.1371/journal.pone.0009157.
Dudd, S.N., Evershed, R.P., Gibson, A.M., 1999. Evidence for varying patterns of exploitation of animal products in different prehistoric pottery traditions based on lipids preserved in surface and absorbed residues. J. Archaeol. Sci. 26, 1473–1482.
Evershed, R.P., Dudd, S.N., Copley, M.S., Mutherjee, A., 2002. Identification of animal fats via compound specific $\delta^{13}C$ values of individual fatty acids: assessments of results for reference fats and lipid extracts of archaeological pottery vessels. Doc. Praehist. 29, 73–96. https://doi.org/10.4312/dp.29.7.
Frak, E., Millard, P., Le Roux, X., Guillaumie, S., Wendler, R., 2002. Coupling sap flow velocity and amino acid concentrations as an alternative method to ^{15}N labelling for quantifying nitrogen remobilization by walnut trees. Plant Physiol. 130, 1043–1053. https://doi.org/10.1104/pp.002139.
Galván, B., Hernandez, C.M., Mallol, C., Mercier, N., Sistiaga, A., Soler, V., 2014. New evidence of early neanderthal disappearance in the Iberian peninsula. J. Hum. Evol. 75, 16–27. https://doi.org/10.1016/j.jhevol.2014.06.002.
García Moreno, A., Rios Garaizar, J., Marín Arroyo, A.B., Ortíz, J.E., de Torres, T., López-Dóriga, I., 2014. La secuencia musteriense de la Cueva del Niño (Aýna, Albacete) y el poblamiento neandertal en el sureste de la península Ibérica. Trab. Prehist. 71, 221–241.
Goodman, K.J., Brenna, J.T., 1992. High sensitivity tracer detection using high-precision gas chromatography-combustion isotope ratio mass spectometry and highly enriched [U-^{13}C]-labelled precursors. Anal. Chem. 64, 1088–1095. https://doi.org/10.1021/ac00034a004.
Goldberg, P., Miller, C., Schiegl, S., Ligouis, B., Berna, F., Conard, N.J., Wadley, L., 2009. Bedding, hearths, and site maintenance in the middle stone age of Sibudu Cave, KwaZulu-natal, South Africa. Archaeol. Anthrop. Sci. 1, 95–122. https://doi.org/10.1007/s12520-009-0008-1.
Grosjean, E., Logan, G.A., 2007. Incorporation of organic contaminants into geochemical samples and an assessment of potential sources: examples from Geoscience Australia marine survey S282. Org. Geochem. 38 (6), 853–869. https://doi.org/10.1016/j.orggeochem.2006.12.013.
Hall, G., Wadley, L., Woodborne, S., 2014. Past environmental proxies from the middle stone age at Sibudu, Kwazulu-natal, South Africa. J. Afr. Archaeol. 12. https://doi.org/10.3213/2191-5784-10246.
Henry, A.G., 2017. Neanderthal cooking and the costs of fire. Curr. Anthropol. 58 (16), S329–S336.
Hobbie, E.A., Werner, R., 2004. Intramolecular, compound-specific, and bulk carbon isotope patterns in C3 and C4 plants: a review and synthesis. New Phytol. 161, 371–385. https://doi.org/10.1016/j.mseb.2011.05.037.
Hockett, B., Haws, J.A., 2002. Taphonomic and methodological perspectives of Leporid hunting during the upper paleolithic of the western Mediterranean. J. Archaeol. Method Theory 9 (3), 269–302.
Ishiwatarii, R., Sugawara, S., Machirara, T., 1992. Long-chain aliphatic nitriles in pyrolysates of young kerogen: implications for the intermediates in petroleum hydrocarbon formation. Geochem. J. 26, 137–146.
Jambrina-Enríquez, M., Herrera-Herrera, A.V., Mallol, C., 2018. Wax lipids in fresh and charred anatomical parts of the Celtis australis tree: insights on paleofire interpretation. Org. Geochem. 122, 147–160. https://doi.org/10.1016/j.orggeochem.2018.05.017.
Karkanas, P., Shahack-Gross, R., Ayalon, A., Bar-Matthews, M., Barkai, R., et al., 2007. Evidence for habitual use of fire at the end of the Lower Paleolithic: site formation processes at Qesem Cave, Israel. J. Hum. Evol. vol. 53, 197–212.
Keeling, R.F., Piper, S.C., Bollenbacher, A.F., Walker, S.J., 2010. Monthly atmospheric $^{13}C/^{12}C$ isotopic ratios for 11 SIO Stations (1977-2008). In: Trends: A Compendium of Data on Global Change. Carbon Dioxide Information Analysis Center. Oak Ridge National Laboratory, U.S. Department of Energy, Oak Ridge, Tenn., U.S.A. https://doi.org/10.3334/CDIAC/ATG.025.
Leierer, L., Jambrina-Enríquez, M., Herrera-Herrera, A.V., Connolly, R., Hernández, C.M., Galván, B., Mallol, C., 2019. Insights into the timing, intensity and natural setting of Neanderthal occupation from the geoarchaeological study of combustion structures: a micromorphological and biomarker investigation of El Salt, unit Xb, Alcoy, Spain. PLoS One. https://doi.org/10.1371/journal.pone.0214955.
Lejay, M., Alexis, M., Quénéa, K., Sellami, F., Bon, F., 2016. Organic signatures of fireplaces: experimental references for archaeological interpretations. Org. Geochem. 99, 67–77. https://doi.org/10.1016/j.orggeochem.2016.06.002.
Lucquin, A., Gibbs, K., Uchiyama, J., Saul, H., Ajimoto, M., Eley, Y., Radini, A., Heron, C.P., Shoda, S., Nishida, Y., Lundy, J., Jordan, P., Isaksson, S., Craig, O.E., 2016. Ancient lipids document continuity in the use of early hunter–gatherer pottery through 9,000 years of Japanese prehistory. Proc. Natl. Acad. Sci. 113 (15), 3991–3996. https://doi.org/10.1073/pnas.1522908113.
Lucquin, A., Robson, H.K., Eley, Y., Shoda, S., Veltcheva, D., Gibbs, K., Heron, C.P., Isaksson, S., Nishida, Y., Taniguchi, Y., Nakajima, S., Kobayashi, K., Jordan, O., Kaner, S., Craig, O.E., 2018. The impact of environmental change of the use of early pottery by East Asian hunter-gatherers. Proc. Natl. Acad. Sci. U. S. A. 115 https://doi.org/10.1073/pnas.1803782115, 7931–793.
Machado, J., Hernández, C.M., Mallol, C., Galván, B., 2013. Lithic production, site formation and Middle Palaeolithic palimpsest analysis: in search of human occupation episodes at Abric del Pastor Stratigraphic Unit IV (Alicante, Spain). J. Archaeol. Sci. 40, 2254–2273. https://doi.org/10.1016/j.jas.2013.01.002.
Mallol, C., Hernández, C.M., Cabanes, D., Sistiaga, A., Machado, J., Rodríguez, A., Pérez, L., Galván, B., 2013. The black layer of Middle Palaeolithic combustion structures. Interpretation and archaeostratigraphic implications. J. Archaeol. Sci. 40, 2515–2537. https://doi.org/10.1016/j.jas.2012.09.017.
Mallol, C., Mentzer, S., Miller, C., 2017. Combustion features. In: Nicosia, C., Stoops, G. (Eds.), Archaeological Soil and Sediment Micromorphology. Wiley, pp. 299–326.
McCarroll, D., Loader, D.J., 2004. Stable isotopes in tree rings. Quat. Sci. Rev. 23 (7–8), 771–801. https://doi.org/10.1016/j.quascirev.2003.06.017.
March, R.J., 2013. Searching for the functions of fire structures in Eynan (Mallaha) and their formation processes: a geochemical approach. In: Bar-Yosef, O., Valla, F.R. (Eds.), Natufian Foragers in the Levant: Terminal Pleistocene Social Changes in Western Asia, Archaeological Series, International Monographs in Prehistory. Ann Arbor, MI, pp. 227–283.
Messager, E., Badou, A., Fröhlich, F., Deniauz, B., Lordkipanidze, D., Voinchet, P., 2010. Fruit and seed biomineralization and its effect on preservation. Archaeol. Anthropol. Sci. 2, 25–34. https://doi.org/10.1007/s12520-010-0024-1.
Millard, P., Grelet, G.A., 2010. Nitrogen storage and remobilization by trees: ecophysiological relevance in a changing world. Tree Physiol. 30, 1083–1095. https://doi.org/10.1093/treephys/tpq042.
Miller, C.E., Goldberg, P., Berna, F., 2013. Geoarchaeological investigations at Diepkloof Rock Shelter, Western Cape, South Africa. J. Archaeol. Sci. 40, 3432–3452. https://doi.org/10.1016/j.jas.2013.02.014.
Morley, M.W., 2007. Mediterranean Quaternary Rockshelter Sediment Records: A Multi-Proxy Approach to Environmental Reconstruction. Ph.D. dissertation. Department of Geography, School of Environment and Development, Faculty of Humanities, University of Manchester.
Oros, D.R., Simoneit, B.R.T., 2001a. Identification and emission factors of molecular tracers in organic aerosols from biomass burning Part 2. Deciduous trees. Appl. Gochem. 16 (13), 1545–1565. https://doi.org/10.1016/S0883-2927(01)00022-1.
Oros, D.R., Simoneit, B.R.T., 2001b. Identification and emission factors of molecular tracers in organic aerosols from biomass burning Part 1. Temperate climate conifers. Appl. Geochem. 16 (13), 1513–1544. https://doi.org/10.1016/S0883-2927(01)00021-X.
Pedentchouk, N., Summer, W., Tipple, B., Pagani, M., 2008. $\delta^{13}C$ and δD composition of n-alkanes from modern angiosperms and conifers: an experimental set up in central Washington State, USA. Org. Geochem. 39, 1066–1071. https://doi.org/10.1016/j.orggeochem.2008.02.005.
Pérez, L., 2014. La gestión de los recursos animales en los Valles de Alcoy durante el Pleistoceno Superior (MIS 3) Estudio zooarqueológico y tafonómico, Universitat Rovira i Virgili, Tarragona. Master Thesis.
Pérez, L.J., 2015. Aproximación experimental a los indicadores de desocupación humana en yacimientos del Pleistoceno superior a partir de los restos termoalterados de conejo. In: Serra, A.S., Pascual, J.L. (Eds.), Preses Petites I Grups Humans En El Passat. II Jornades D'arqueozoologia. Museu de Prehistòria de València, Valencia, pp. 27–46.
Post-Beittenmiller, D., 1996. Biochemistry and molecular biology of wax production in plants. Annu. Rev. Plant Physiol. Plant Mol. Biol. 47, 405–430. https://doi.org/10.1146/annurev.arplant-47-1-405.
Recio, C., Martín, Q., Raposo, C., 2013. GC-C-IRMS analysis of FAMEs as a tool to ascertain the diet of Iberian pigs used for the production of pork products with high added value. Grasas Aceites 64 (2), 181–190. https://doi.org/10.3989/gya.130712.
Roebroeks, W., Villa, P., 2011. On the earliest evidence for habitual use of fire in Europe. Proc. Natl. Acad. Sci. U.S.A. 108, 5209–5214. https://doi.org/10.1073/pnas.1018116108.
Rodríguez-Cintas, A., Cabanes, D., 2015. Phytolith and FTIR studies applied to combustion structures: the case of the middle paleolithic site of el Salt (Alcoy, Alicante). Quat. Int. 431A, 16–26. https://doi.org/10.1016/j.quaint.2015.09.043.
Rogge, W.E., Hildemann, L.M., Mazurek, M.A., Cass, G.R., 1991. Sources of fine organic aerosol. 1. Charbroilers and meat cooking operations. Environ. Sci. Technol. 25, 1112–1125. https://doi.org/10.1021/es00018a015.
Simoneit, B.R.T., Rushdi, A.I., bin Abas, M.R., Didyk, B.M., 2003. Alkyl amides and nitriles as novel tracers for biomass burning. Environ. Sci. Technol. 37 (1), 16–21. https://doi.org/10.1021/es020811y.
Steele, V.J., Stern, B., Stott, A.W., 2010. Olive oil or lard?: distinguishing plant oils from animal fats in the archaeological record of the eastern Mediterranean using gas chromatography/combustion/isotope ratio mass spectrometry. Rapid Commun. Mass Spectrom. 24, 3478–3484. https://doi.org/10.1002/rcm.4790.
Spangenberg, J.E., Ogrinc, N., 2001. Authentication of vegetable oils by bulk and molecular carbon isotope analyses with emphasis on olive oil and pumpkin seed oil. Agric. Food Chem. 49, 1534–1540. https://doi.org/10.1021/jf001291y.
Spangenberg, J.E., Jacomet, S., Schibler, J., 2006. Chemical analyses of organic residues in archaeological pottery from Arbon Bleiche 3, Switzerland - evidence for dairying in the Late Neolithic. J. Archaeol. Sci. 33, 1–13. https://doi.org/10.1016/j.jas.2005.05.013.
Sytsma, K.J., Morawetz, G., Pires, J.C., Nepokroeff, M., Conti, E., Zjhra, M., Hall, J.C.,

Chase, M.W., 2002. Urticalean rosids: circumscription, rosid ancestry, and phylogenetics based on rbcL, trnL-F, and ndhF sequences. Am. J. Bot. 89, 1531–1546. https://doi.org/10.3732/ajb.89.9.1531.

Taché, K., Craig, O., 2015. Cooperative harvesting of aquatic resources and the beginning of pottery production in north-eastern North America. Antiquity 89, 177–190. https://doi.org/10.15184/aqy.2014.36.

Thevenon, F., Bard, E., Williamson, D., Beaufort, L., 2004. A biomass burning record from the West Equatorial Pacific over the last 360 ky: methodological, climatic and anthropic implications. Palaeogeogr. Palaeoclimatol. Palaeoecol. 213, 83–99.

Vidal-Matutano, P., Pérez-Jordà, G., Hernández, C.M., Galván, B., 2018. Macrobotanical evidence (wood charcoal and seeds) from the Middle Palaeolithic site of El Salt, Eastern Iberia: palaeoenvironmental data and plant resources catchment areas. J. Archaeol. Sci. Rep. 19, 454–464. https://doi.org/10.1016/j.jasrep.2018.03.032.

Wadley, L., Sievers, C., Bamford, M., Goldberg, P., Berna, F., Miller, C., 2011. Middle Stone Age bedding construction and settlement patterns at Sibudu, South Africa. Science 334, 1388–1391. https://doi.org/10.1126/science.1213317.

Wang, J., Simoneit, B.R.T., Sheng, G., Chen, L., Xu, L., Wang, X., Wang, Y., Sun, L., 2017. The potential of alkyl amides as novel biomarkers and their application to paleocultural deposits in China. Sci. Rep. 7 https://doi.org/10.1038/s41598-017-15371-z.

Wiesenberg, G.L.B., Schwarzbauer, J., Schmidt, M.W.I., Schwark, L., 2004. Source and turnover of organic matter in agricultural soils derived from n-alkane/n-carboxylic acid compositions and C-isotope signatures. Org. Geochem. 35, 1371–1393. https://doi.org/10.1016/j.orggeochem.2004.03.009.

Woodbury, S.E., Evershed, R.P., Rossell, J.B., 1998. $\delta^{13}C$ analyses of vegetable oil fatty acid components, determined by gas chromatography-combustion-isotope ratio mass spectrometry, after saponification or regiospecific hydrolysis. J. Chromatogr. A 805 (1–2), 249–257.

Wrangham, R., 2017. Control of fire in the paleolithic: evaluating the cooking hypothesis. Curr. Anthropol. 58. S000-S000. 10.1086/692113.